



Review

Review of Energy Storage Capacitor Technology

Wenting Liu ^{1,2}, Xianzhong Sun ^{1,2,3,4,*} Xinyu Yan ⁵, Yinghui Gao ^{1,2,3,4}, Xiong Zhang ^{1,2,3,4} Kai Wang ^{1,2,3,4} and Yanwei Ma ^{1,2,3,4,*}

¹ Institute of Electrical Engineering, Chinese Academy of Sciences, Beijing 100190, China; liuwenting23@mails.ucas.ac.cn (W.L.); gyh@mail.iee.ac.cn (Y.G.); zhangxiong@mail.iee.ac.cn (X.Z.); wangkai@mail.iee.ac.cn (K.W.)

² University of Chinese Academy of Sciences, Beijing 100049, China

³ Key Laboratory of High Density Electromagnetic Power and Systems (Chinese Academy of Sciences), Haidian District, Beijing 100190, China

⁴ Shandong Key Laboratory of Advanced Electromagnetic Conversion Technology, Institute of Electrical Engineering and Advanced Electromagnetic Drive Technology, Qilu Zhongke, Jinan 250013, China

⁵ TBEA Sunoasis Co., Ltd., Xi'an 830011, China; 13649270712@163.com

* Correspondence: xzsun@mail.iee.ac.cn (X.S.); ywma@mail.iee.ac.cn (Y.M.)

Abstract: Capacitors exhibit exceptional power density, a vast operational temperature range, remarkable reliability, lightweight construction, and high efficiency, making them extensively utilized in the realm of energy storage. There exist two primary categories of energy storage capacitors: dielectric capacitors and supercapacitors. Dielectric capacitors encompass film capacitors, ceramic dielectric capacitors, and electrolytic capacitors, whereas supercapacitors can be further categorized into double-layer capacitors, pseudocapacitors, and hybrid capacitors. These capacitors exhibit diverse operational principles and performance characteristics, subsequently dictating their specific application scenarios. To make informed decisions in selecting capacitors for practical applications, a comprehensive knowledge of their structure and operational principles is imperative. Consequently, this review delved into the structure, working principles, and unique characteristics of the aforementioned capacitors, aiming to clarify the distinctions between dielectric capacitors, supercapacitors, and lithium-ion capacitors.



Citation: Liu, W.; Sun, X.; Yan, X.; Gao, Y.; Zhang, X.; Wang, K.; Ma, Y. Review of Energy Storage Capacitor Technology. *Batteries* **2024**, *10*, 271. <https://doi.org/10.3390/batteries10080271>

Academic Editor: Johan E. ten Elshof

Received: 23 June 2024

Revised: 21 July 2024

Accepted: 25 July 2024

Published: 29 July 2024



Copyright: © 2024 by the authors. Licensee MDPI, Basel, Switzerland. This article is an open access article distributed under the terms and conditions of the Creative Commons Attribution (CC BY) license (<https://creativecommons.org/licenses/by/4.0/>).

1. Introduction

Due to global economic growth and expanding population, there has been a consistent and unwavering increase in the demand for energy [1]. The extensive exploitation of fossil fuels, however, has resulted in numerous challenges, including global warming and environmental pollution [2]. These issues not only pose a direct threat to human health but also inflict significant damage on our ecosystems. Furthermore, given the limited reserves of fossil fuels, the issue of energy scarcity is rapidly escalating [3]. Consequently, there is an urgent need to move away from traditional fossil fuels and explore renewable energy sources. However, renewable energy sources such as solar energy, wind energy, tidal energy, and geothermal energy are inherently intermittent and unstable, posing challenges to their utilization [4,5]. To enhance the utilization of renewable energy, it is imperative to transform it into other forms, primarily electricity, for storage. Consequently, the advancement of energy storage technology holds immense significance in optimizing energy structures, enhancing energy efficiency, safeguarding energy security, and fostering sustainable energy development.

For over two centuries, batteries have been extensively utilized for energy storage purposes and continue to be so today. In recent years, lithium-ion batteries with polymer

solid-state electrolytes have received increasing attention due to their inherent safety and excellent thermal stability, promising large-scale applications [6]. Furthermore, various other technologies such as solid oxide fuel cells (SOFCs), electrochemical capacitors (ECs), superconducting magnetic energy storage (SMES) systems, flywheel energy storage systems, and dielectric capacitors are also commonly employed for storing energy [7]. Capacitors possess higher charging/discharging rates and faster response times compared with other energy storage technologies, effectively addressing issues related to discontinuous and uncontrollable renewable energy sources like wind and solar [3]. Furthermore, they can tackle challenges such as peak shaving, frequency regulation, and intelligent power supply within the power grid, thereby enhancing the efficiency of multi-energy coupling and promoting energy conservation and emission reduction [8]. With the rapid development of the electronics industry, capacitors have undergone an evolution from relatively primitive forms such as air-dielectric capacitors, mica-dielectric capacitors, and paper-dielectric capacitors to ceramic-dielectric capacitors and electrolytic capacitors [9]. The advent of diverse dielectric materials, especially organic media, combined with sophisticated manufacturing techniques, has led to a significant reduction in capacitors' overall size and a remarkable boost in performance. In recent years, the emergence of the double-layer theory has fueled the rise of supercapacitors, with double-layer supercapacitors and hybrid supercapacitors experiencing rapid growth and exhibiting promising applications [10]. The performance of different capacitors is shown in Table 1, and the comparison chart of energy density and power density for different capacitors is shown in Figure 1.

Table 1. Performance comparison of different capacitors.

Type	High Capacitance	High Voltage	Rate Performance	Cycle Stability	Cost	Polarity	Life Time	Main Purpose	Electrode Material
Film capacitor	☒	□	□	○	△	non-existent	□	improve frequency and absorb power supply noise	metal foil or metalized film
Aluminum electrolytic capacitor	○	○	△	△	□	exist	△	smoothing and decoupling	aluminum foil (cathode/anode)
tantalum electrolytic capacitor	○	△	○	△	△	exist	○	coupling and decoupling	Ta (anode) MnO ₂ (cathode)
Ceramic capacitor	△	○	□	□	○	non-existent	□	coupling and decoupling	metals such as silver and copper
EDLC	□	☒	☒	△	☒	exist	△	backup power	carbon-based materials (anode/cathode)
Lithium-ion Capacitor	□	☒	☒	△	☒	exist	☒	backup power and energy storage applications	carbon-based materials (positive/negative electrode)

□: excellent; ○: good; △: not good; ☒: bad.

As new energy technology and capacitor energy storage continue to evolve, users may encounter numerous questions related to capacitors. To make informed decisions about their selection and usage, it is imperative to gain a comprehensive understanding of capacitors' structure and operating principles. Furthermore, there are some new researchers in the realm of capacitor energy storage who lack a thorough comprehension of capacitors' classification, structure, and operational mechanisms, which can readily lead to confusion regarding the various types of capacitors. Hence, this review endeavors to offer a comprehensive overview of the structures and operational principles of various capacitor types. Its objective is to illuminate the distinctions between dielectric capacitors,

supercapacitors, and lithium-ion capacitors, thereby facilitating a thorough understanding of these capacitor categories among the readership.

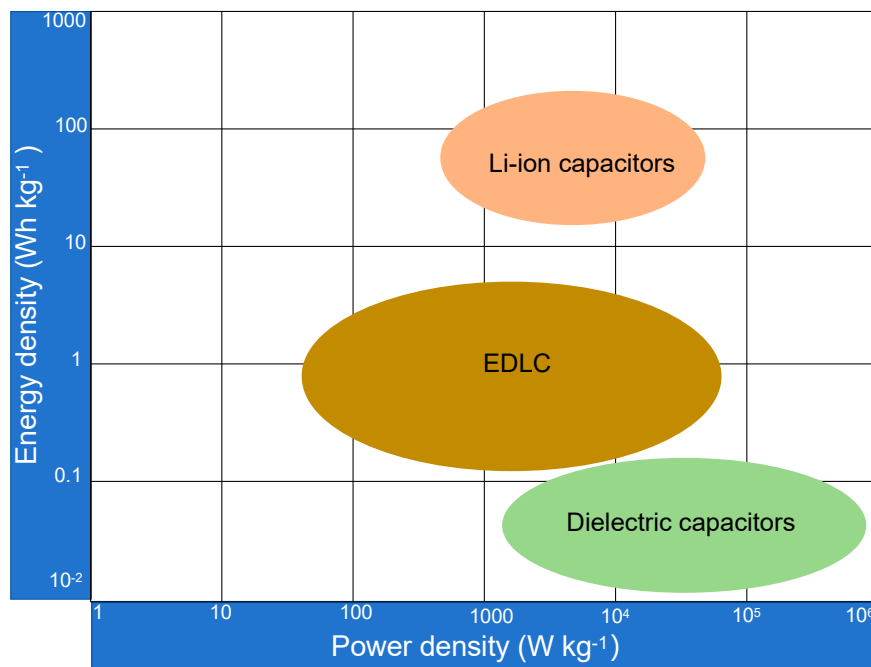


Figure 1. The comparison chart of energy density and power density for different capacitors. Reproduced from Ref. [11] with permission.

2. Dielectric Capacitor

The development of commercial dielectric capacitors can be traced back to 1876 when Fitzgerald invented the wax-impregnated paper dielectric capacitor equipped with foil electrodes [12]. This innovation was swiftly adopted in early radio-receiving equipment, significantly advancing radio communication technology. Subsequently, in 1909, William Dubilier introduced the mica dielectric capacitor, injecting new vitality into the field of radio transmission. Around 1926, capacitors based on titanium dioxide hit the market, further diversifying the types and enhancing the performance of capacitors. Then, in 1936, Cornell-Dubilier successfully commercialized aluminum electrolytic capacitors, launching a series of commercial products that marked a new era in the development of aluminum electrolytic capacitor technology. With the discovery of barium titanate in 1941, researchers embarked on the study of barium titanate-based dielectric capacitors, further advancing capacitor technology. During World War II, significant breakthroughs were made in capacitor manufacturing technology. Bosch leveraged lacquered paper and vacuum metallization techniques to mature the metalized paper capacitor, significantly enhancing its performance [13]. In 1954, Bell Labs successfully developed the first metalized polymer film capacitor, rejuvenating the capacitor industry [14]. From the 1970s to the 1980s, significant progress was made in the manufacture of multilayer ceramic capacitors (MLCCs) through the adoption of tape-casting technology and co-firing of ceramic electrodes. This resulted in a substantial increase in capacitance values and voltage withstand capabilities, vastly expanding the application areas of ceramic capacitors and making them indispensable components in numerous electronic devices. Currently, the primary types of dielectric capacitors include film capacitors, electrolytic capacitors, and ceramic capacitors [15].

The capacitance value of a capacitor is typically determined using Equation (1) [16]:

$$C = \frac{\epsilon_0 \epsilon_r A}{D} \quad (1)$$

where ϵ_r is the dielectric constant with respect to the electrolyte utilized, ϵ_0 is the permittivity of the vacuum, A is the surface area of the electrode material accessible to the electrolyte ions, and D is the effective thickness (charge separation distance) between the electrodes.

Therefore, the capacitance value can be increased by increasing the surface area of the electrodes and decreasing the distance between them.

In comparison to various electrical storage devices like batteries, dielectric capacitors possess the capability to discharge stored energy in an extremely brief timeframe (microseconds), resulting in the generation of substantial power pulses [17]. Their rapid charging and discharging rates render them ideally suited for high-power/pulse power systems, including medical defibrillators, pulsed lasers, power conditioning systems, and advanced electromagnetic emission systems [18–21]. Additionally, they are effective in harnessing energy from intermittent renewable sources [22]. However, the relatively low energy density of dielectric capacitors poses significant constraints on the miniaturization and lightweighting of equipment [23]. If the energy density of dielectric capacitors could be enhanced, it would lead to a substantial broadening of their application scope in the realm of energy storage.

The energy storage mechanism of a dielectric relies on its polarization process triggered by an electric field [24]. When an electric field is applied, the dielectric becomes polarized, leading to the accumulation of equal amounts of positive and negative charges on its surface. Consequently, energy is stored within the dielectric in the form of an electric field, as shown in Figure 2. The mechanism behind energy storage and release in dielectrics is elucidated through the electric displacement (D)-electric field (E) loop. As an electric field is applied, dielectrics become polarized due to the relative displacement of oppositely charged particles within their dipoles. Conversely, upon the removal of the electric field, depolarization occurs, causing the oppositely charged centers to tend toward overlap [25].

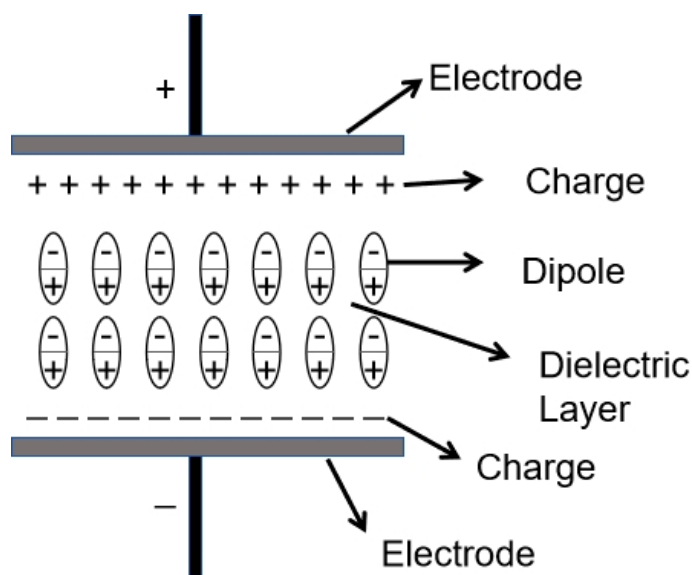


Figure 2. A schematic depiction of an electrically charged dielectric capacitor reveals how the charges of oriented electric dipoles, under the influence of a bias, contribute to binding the opposite charges at their respective electrode interfaces.

Dielectric capacitors can be categorized into several types, including film capacitors without electrolytes, electrolytic capacitors that utilize electrolytes, and ceramic capacitors. Film capacitors are made by depositing metal layers with different patterns on both sides of a thin film. While they can achieve voltages of tens of thousands of volts per unit, their capacitance is relatively small, necessitating parallel connection for high-power applications. Electrolytic capacitors can be classified into aluminum electrolytic capacitors (with an anode made of aluminum oxide, a separator of fibrous paper for insulation and electrolyte

absorption, and an electrolyte typically composed of boric acid, ammonia water, and ethylene glycol) and tantalum electrolytic capacitors (with an anode made of tantalum pentoxide and a separator of fibrous paper). Typically, the voltage rating of a single unit is ≤ 100 V (low-voltage electrolytic capacitor) or ≥ 100 V (high-voltage electrolytic capacitor). Under high voltage conditions, they need to be used in series. Ceramic capacitors can be categorized into ceramic disc capacitors and multilayer ceramic capacitors. These capacitors are compact and cost-effective and possess excellent electrical properties, leading to their widespread application. In particular, high-capacity multilayer ceramic capacitors have been used to replace more expensive tantalum capacitors.

2.1. Film Capacitor

Film capacitors, alternatively known as plastic film capacitors, frequently employ metal foil as electrodes and plastic film as the dielectric. These capacitors often incorporate artificially synthesized polymer materials as dielectrics, enabling the selection of appropriate dielectric materials based on specific requirements, thereby exhibiting immense development potential. Recently, research in the field of film capacitors has focused on optimizing their dielectric properties. Meng et al. [26] proposed a hierarchical structural design approach to enhance the dielectric properties of metalized polypropylene (PP) film capacitors by utilizing terephthalaldehyde. This method offers insights into improving the dielectric properties of PP films by regulating charge transport behavior. Hu et al. [27] developed an ultra-high-temperature capacitor with relaxor ferroelectric (RFE) films by controlling polarization behavior. They further suggested that adjusting the intrinsic/extrinsic polarization ratio can enhance energy storage performance, providing a feasible approach to improving the high-temperature performance and dielectric strength of capacitors.

Film capacitors can be classified based on their structure, type of dielectric, and electrode formation method. To begin with, film capacitors are produced either in the form of winding utilizing a capacitor winding machine or as stacks of dielectric films [28]. These two distinct manufacturing methods are commonly referred to as coil technology and the stacking technique, respectively [29,30]. Therefore, based on their structure, film capacitors can be broadly classified into two types: “wound type” and “stacked type”. The digital images are shown in Figure 3. The wound type involves winding and stamping polymer films and then inserting them into a shell. This type can further be divided into two winding methods: inductive (Figure 4a) and non-inductive (Figure 4b). The stacked type, on the other hand, involves stacking multiple layers of polymer films together and then inserting the stacked body into a shell (Figure 4c). Currently, wound-type film capacitors are more commonly used due to their ease of manufacturing.

Furthermore, film capacitors can be categorized into paper media and organic media based on their insulation materials. Paper dielectric capacitors are a type of wound capacitor that employs capacitor paper as the insulating medium and aluminum foil as the electrode. These capacitors consist of two or more layers of aluminum sheets interspersed with paper sheets. The paper sheets serve as the dielectric, whereas the aluminum sheets function as the capacitor electrodes, as shown in Figure 5a [31]. During the manufacturing process, paper and aluminum sheets are typically rolled into cylindrical shapes, with leads attached to both ends of the aluminum sheet, as depicted in Figure 5b. Subsequently, the entire cylindrical structure is coated with a protective layer of wax or plastic resin to safeguard it from exposure to moisture in the air.

Compared with traditional paper dielectric capacitors, the manufacturing process of metalized paper capacitors is more distinctive. It employs vacuum evaporation technology to deposit an ultra-thin and even layer of zinc or aluminum film onto the surface of the paper. Following this, the paper coated with this metal film is wound into a cylindrical structure, completing the overall fabrication of the metalized capacitor. Metalized paper capacitors feature a direct and thin coating of aluminum on paper, resulting in a thinner aluminum layer compared with traditional paper capacitors. This thinner layer contributes to a smaller capacitor size. Paper dielectric capacitors offer a diverse range of capacitance

and operating voltage, along with a straightforward manufacturing process, low cost, and ease of metallization. Owing to these attributes, they are commonly utilized in high-voltage and high-current applications.



Figure 3. The digital images of film capacitors. (a) Wound-type film capacitors. (b) Stacked-type film capacitors. The capacitor on the left is used for DC circuits, while the one on the right is used for AC circuits.

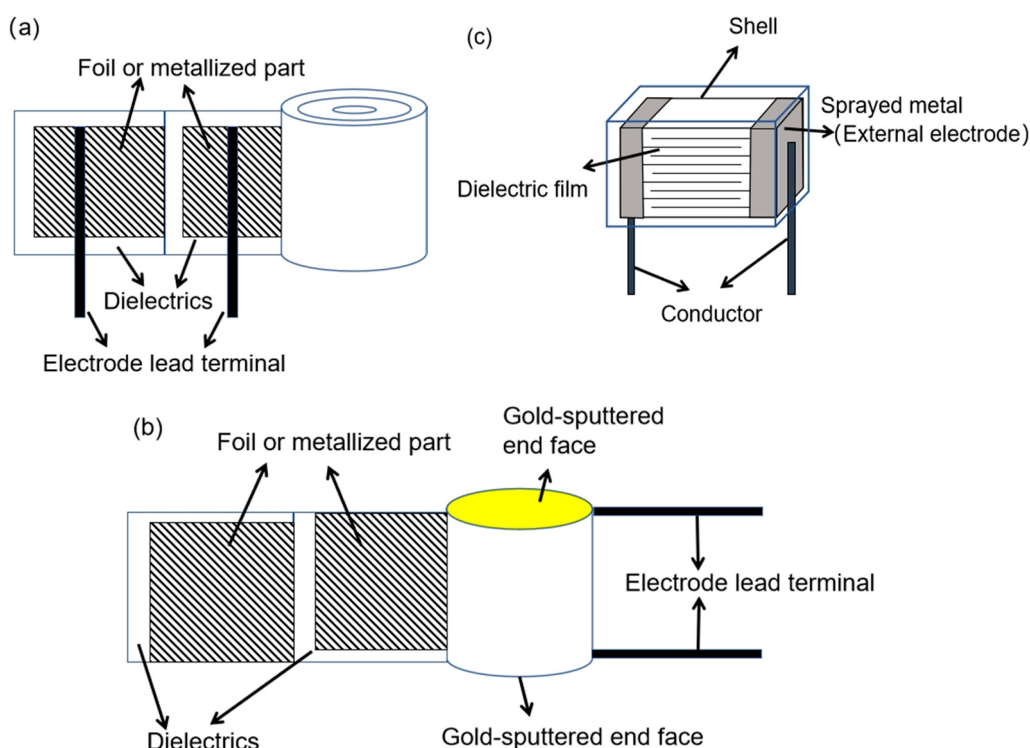


Figure 4. The structural diagram of film capacitors. (a) Inductive winding method. (b) Non-inductive winding method. (c) Stacked film capacitor.

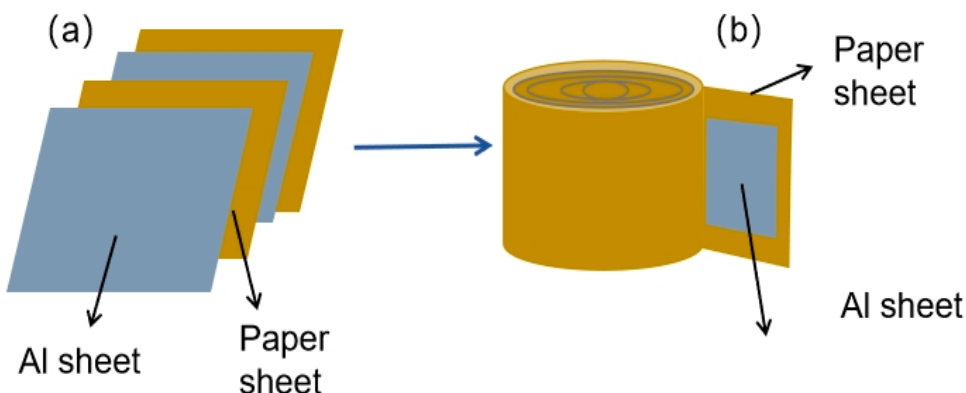


Figure 5. (a) Assembly of a paper sheet capacitor. (b) The process of rolling up a paper sheet capacitor into a cylinder. Reproduced from Ref. [31] with permission.

Organic dielectric capacitors primarily consist of synthetic organic thin films serving as dielectric materials and are typically constructed in a wound structure. Common dielectric materials employed in these capacitors include polypropylene (PP), polyethylene terephthalate (PET), polyethylene naphthalate (PEN), polyphenylene sulfide (PPS), and polycarbonate (PC) [28,32–34]. Ran et al. [35] improved the micro-morphology of PP films by utilizing an organic crystallization accelerator with good dispersion. The film capacitors produced using this method exhibit excellent breakdown strength. Ping et al. [36] prepared a double-layer polymer film by solution casting on the surface of PET film and coating it with boron nitride nanosheets. The resulting film capacitor exhibits excellent breakdown strength (736 MV m^{-1}) and high energy density (8.77 J cm^{-3}). Zou et al. [37] developed a high-performance thin-film capacitor through the controlled deposition of Si_3N_4 on PEN. This capacitor film possesses excellent mechanical properties, making it a promising candidate for power converters in electric vehicles. Zhang et al. [38] designed and prepared a P-3-P sandwich structured film with PC as the outer insulation layer and 3 wt% TiO_2 –PC/polyvinylidene fluoride as the middle polarization layer using solution casting and hot-pressing processes. This film exhibits excellent charge-discharge characteristics, offering a promising possibility for the construction of high-energy storage film capacitors.

In comparison to inorganic dielectric capacitors, organic dielectric capacitors primarily utilize polymer materials as dielectrics, benefiting from the abundance of raw materials available. Additionally, the thickness of the films can be made exceptionally thin. Nevertheless, organic media are susceptible to aging and exhibit limited heat resistance, potentially compromising the capacitors' performance [39,40]. The characteristics of film capacitors vary significantly depending on the type of dielectric medium used, resulting in diverse application fields. Organic dielectric capacitors can be classified into two electrode types: metal foil electrodes (the foils are typically on the order of $6 \mu\text{m}$ in thickness) and metalized electrodes (the metalized layers are $<100 \text{ nm}$ thick) [41]. The organic dielectric capacitor of a metal foil electrode is made of two layers of plastic film or sheet. Each layer is interspersed with thin aluminum metal foil or sheet, serving as the electrode. Subsequently, the plastic sheets and aluminum sheets are rolled into a cylindrical jelly roll structure. To establish electrical connections, wire leads are attached to both ends of the aluminum sheets, typically through soldering or metal spraying techniques. The thickness of the plastic film determines the separation distance within the capacitor, while the operating area is dictated by the size of the electrodes. In metalized film organic dielectric capacitors, the aluminum sheets or foils are superseded by metal layers that are vacuum-deposited onto the thin film layer. These metal layers possess a thickness of approximately 1/100 of that of the metal foil, making them significantly thinner and more conducive to space conservation [31]. The most frequently utilized metal layer is composed of ultra-thin aluminum. The dielectric is typically formed by a plastic film layer made of synthetic materials, while the electrode is

comprised of an aluminum layer [42]. The schematic diagram of the structure of organic dielectric capacitors is shown in Figure 6.

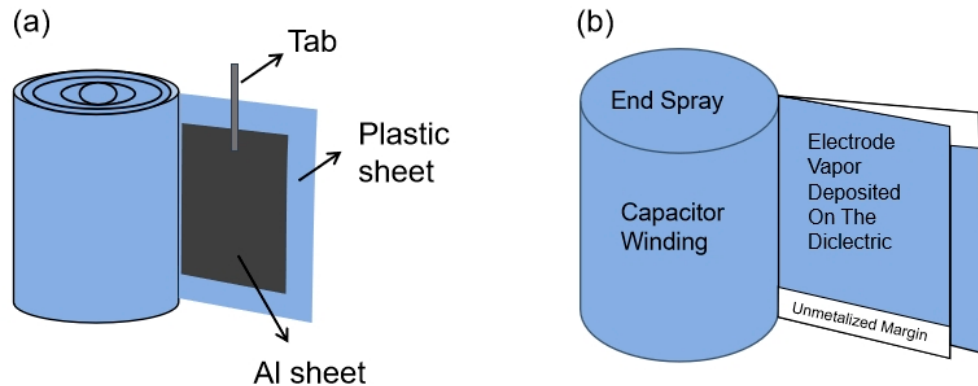


Figure 6. (a) Foil-type organic dielectric capacitor. (b) The capacitor with metalized electrodes, in which the electrodes are typically very thin aluminum layers deposited by vapor deposition onto an organic dielectric.

Finally, film capacitors can be categorized into two types: foil-type film capacitors and metalized film capacitors, depending on their distinct electrode formation techniques. The foil-type film capacitors represent the earliest incarnation of wound capacitors. Typically, they are crafted with clamping aluminum foil, which possesses exceptional ductility, within an insulating medium and then winding it, as shown in Figure 7. Conversely, the electrode of a metalized film capacitor eschews the use of metal foil. Instead, an ultra-thin metal film is deposited onto the capacitor through the process of vacuum evaporation, as shown in Figure 8. Compared with metal foil electrode film capacitors, metalized film capacitors have the obvious advantage of self-healing. Self-healing refers to the phenomenon that when a metalized capacitor experiences breakdown due to defects in the dielectric, an arc current is immediately generated at the breakdown point, and this current density is concentrated at the center of the breakdown point [43,44]. Due to the thin metallization film (less than 0.1 μm), the heat generated by this current is sufficient to melt and evaporate the metal near the breakdown point, forming a metal-free zone around the breakdown area, restoring insulation between the two electrodes of the capacitor, thus restoring normal operation of the capacitor. The self-healing properties of metalized film capacitors enable them to be applied in more complex situations.



Figure 7. (a,b) Overall structural diagram of a disassembled foil-type film capacitor. (c) The aluminum foil is sandwiched between the plastic films.

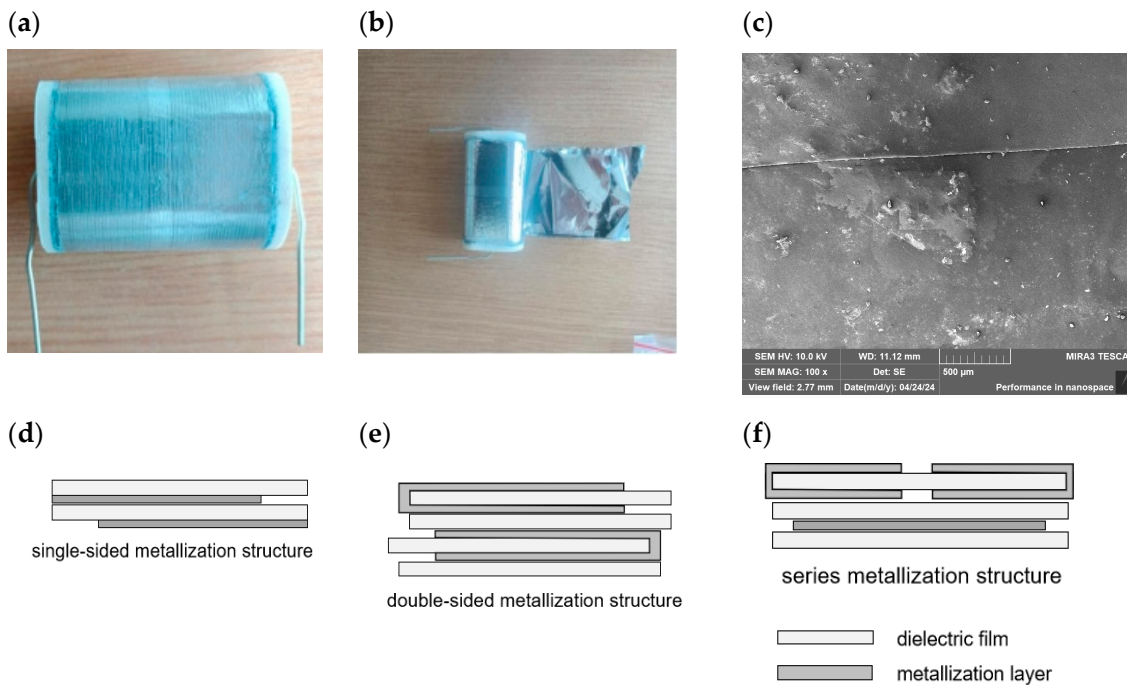


Figure 8. (a,b) Disassembled metalized film capacitor. (c) Placing the dismantled metalized film under a scanning electron microscope (SEM) reveals the deposition of aluminum on the film. (d) Single-sided metallization structure. (e) Double-sided metallization structure. (f) Series metallization structure.

2.2. Electrolytic Capacitor

Electrolytic capacitors are capacitors that exist in two forms: non-polar and polar. The anode of these capacitors typically comprises metal foil, such as aluminum or tantalum, with an oxide film, often aluminum oxide or tantalum pentoxide, serving as the dielectric and adhering closely to the anode. The cathode, on the other hand, consists of a combination of conductive materials, electrolytes (which can be either liquid or solid), and additional materials. The naming of electrolytic capacitors is derived from the electrolyte, which forms the principal component of the cathode. Notably, most electrolytic capacitors exhibit polarity, necessitating the application of voltage with the appropriate polarity. In the event of a reversed connection or incorrect polarity, the capacitor can undergo a short circuit, leading to a significant current flow that may result in permanent damage to the capacitor [31]. Electrolytic capacitors feature a thin dielectric layer, an extensive positive electrode area, and, consequently, a high capacitance per unit volume. This allows them to often boast higher capacitance values compared with other dielectric capacitors. However, they also exhibit a significant leakage current and a relatively short lifespan. When utilizing electrolytic capacitors, it is crucial to adhere to polarity requirements, ensuring that the positive and negative poles are connected correctly to avoid any mishaps.

In recent years, research on electrolytic capacitors has primarily concentrated on electrode materials and production processes. Bai et al. [45] utilized a protective atmosphere sintering process to produce sintered foils with added starch, evaluating the impact of starch addition within the range of 0–50 volume percent on the specific capacitance and anti-buckling performance of the sintered foils. This work unveiled the potential of starch addition in optimizing the properties of sintered foils, providing a valuable reference for developing an advanced powder metallurgy preparation process. Zeng et al. [46] employed additive manufacturing technology to produce anode foils, systematically investigating the influence of aluminum particle size and sintering temperature on the electrical properties of the anode foils. They also discussed the reaction mechanisms during sintering and the inherent relationship between the microstructure and electrical properties of the anode foils. Chen et al. [47] utilized metallic glass (MG) as a binder to adhere Ta powder at low

temperatures (513 K), yielding MG-Ta composites. When applied in tantalum electrolytic capacitors, these composites exhibited a 57% increase in specific capacitance compared with pure Ta materials, accompanied by a 32% enhancement in mechanical properties.

2.2.1. Aluminum Electrolytic Capacitors

Aluminum electrolytic capacitors (AECs) offer a superior cost-to-energy ratio and volume efficiency compared with various other capacitor types [48]. As a result, they are frequently employed at the dc-link of power electronic converters (PECs) to serve as an energy buffer [49]. The physical structure and detailed structure of AEC are shown in Figure 9a. It comprises two aluminum electrodes, with a thin oxide film layer (known as alumina) serving as the dielectric [50]. Additionally, it includes a paper separator and an electrolyte, which is a blend of solvents and additives (shown in Figure 9b) [51].

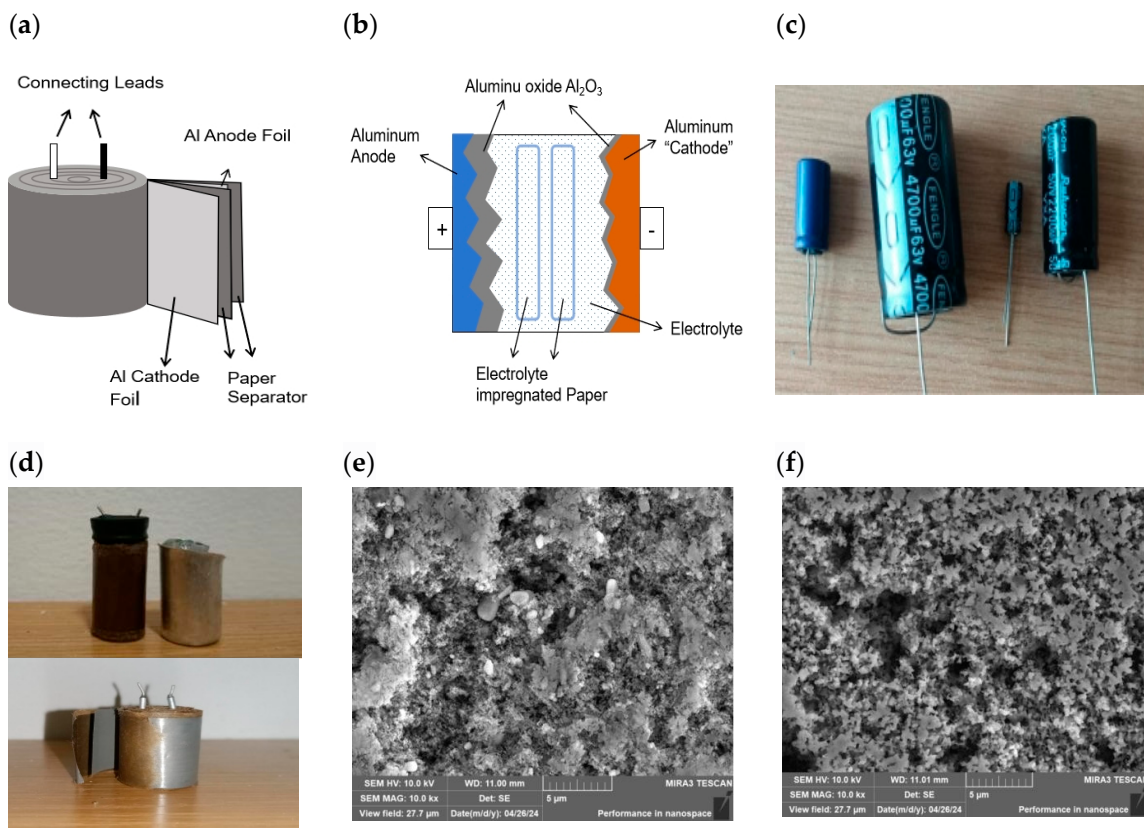


Figure 9. (a) Physical structure of ACE. Reproduced from Ref. [48] with permission. (b) A detailed structural diagram of the AEC, which consists of etched aluminum electrodes, alumina dielectrics, electrolyte carriers, and paper sheets impregnated with the electrolyte. Reproduced from Ref. [50] with permission. (c) Digital images of aluminum electrolytic capacitors. (d) The dismantled aluminum electrolytic capacitor. (e) The image of the anode aluminum foil of the aluminum electrolytic capacitor under a scanning electron microscope reveals that the anode aluminum foil is coated with aluminum oxide. (f) The image of the cathode aluminum foil of the aluminum electrolytic capacitor under a scanning electron microscope reveals that it is an etched aluminum foil.

In aluminum electrolytic capacitors, both the anode and cathode consist of pure aluminum foil. The anode foil is coated with a thin layer of aluminum oxide, electrically insulating in nature, serving as the dielectric. This oxide coating, along with the cathodes, is separated by electrolytic paper soaked in an electrolyte solution. This paper, possessing high porosity, can absorb and hold the maximum amount of electrolyte. While the cathode aluminum foil also possesses a naturally formed, very thin insulating oxide layer due to exposure to air, its thickness is significantly thinner compared with the oxide layer on the

anode foil [52]. The electrolyte serves as the actual cathode of the capacitor when compared to the anode foil, while the cathode foil merely collects current from the electrolyte [48]. Figure 9c shows digital images of aluminum electrolytic capacitors, and the disassembled structure of one of the aluminum electrolytic capacitors is depicted in Figure 9d. After soaking the anode and cathode aluminum foils of the disassembled aluminum electrolytic capacitor in ionized water and allowing them to dry, they were observed under a scanning electron microscope. It can be observed that the anode aluminum foil is coated with aluminum oxide (as shown in Figure 9e), while the cathode aluminum foil is etched aluminum foil (as shown in Figure 9f).

Before forming a layer, the anode foil needs to undergo other processing. Initially, it is etched to enlarge its surface area, enabling better performance [53]. Subsequently, anodization is performed by applying a direct current voltage, resulting in the formation of a thin layer of aluminum oxide on the anode foil's surface. This oxide layer functions as the dielectric in AEC. Conversely, the thin layer of Al_2O_3 present on the cathode results from the natural oxidation of aluminum, which effectively mitigates corrosion.

AEC is a type of polarized capacitor that can only be subjected to a DC bias in one direction. Its electrochemical structure is shown in Figure 10 [48]. The dissociation of water molecules in the electrolyte produces proton (H^+) and hydroxyl (OH^-) ions, which can freely exist in the electrolyte. When a positive electric field is applied to the AEC terminal, staying within the rated voltage, the OH^- ions are drawn toward the aluminum anode foil. However, they encounter a dense dielectric barrier that prevents their passage. Conversely, if the applied negative voltage surpasses the potential hurdle posed by the aluminum oxide formed during passivation, the H^+ ions are drawn toward the anode foil. Given their significantly smaller size compared with OH^- ions, the H^+ ions can effortlessly penetrate the dielectric and arrive at the anode, resulting in the production of hydrogen gas. Meanwhile, the OH^- ions migrate toward the cathode and unite with aluminum (Al^{3+}) ions, leading to the formation of aluminum oxide on the cathode foil. In this case, the cathode capacitance will decrease, thereby reducing the total capacitance. If voltage is applied for a long time, it will damage the capacitor, so the polarity of ACE cannot be reversed.

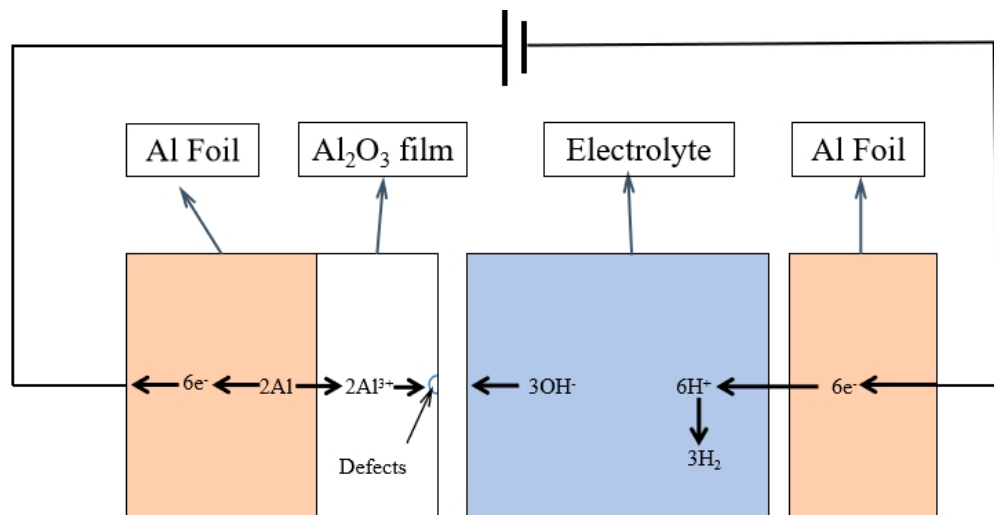


Figure 10. Electrochemical structure of AEC. Reproduced from Ref. [48] with permission.

The manufacturing process of aluminum electrolytic capacitors primarily comprises the following steps, as depicted in Figure 11 [50,54]:

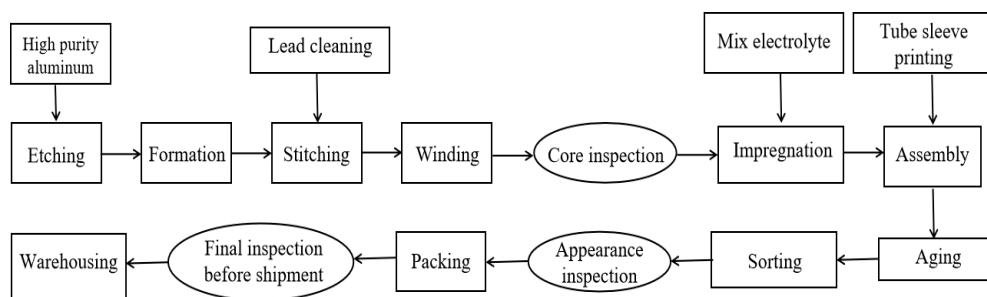


Figure 11. Manufacturing process diagram of aluminum electrolytic capacitors.

- (1) Etching: High-purity aluminum foil undergoes an etching process through an electrochemical method in a chloride solution, utilizing either direct or alternating current. The anode and cathode foils are crafted from virtually pure aluminum foil. To enhance their effective surface area and minimize the size of the capacitor, anode foils ranging from 0.05 to 0.11 mm in thickness and cathode foils measuring 0.02 to 0.05 mm thick are continuously subjected to electrochemical etching in a chloride solution, utilizing either alternating current or direct current. Typically, AC electrolysis is employed for the production of low-voltage capacitors, whereas DC electrolysis is utilized for the fabrication of medium- and high-voltage capacitors.
- (2) Formation: Through electrolysis, a continuous voltage exceeding the nominal value is applied, resulting in the formation of an aluminum oxide layer on the surface of the aluminum foil. The thickness of the alumina dielectric film can be controlled.
- (3) Slitting: After etching and anodizing the aluminum foil roll, the foil is cut into a specified width according to the size of the capacitor shell.
- (4) Winding: Secure the lead-out wires of the anode and cathode foils using rivets or welding and position the foils between isolation plates. Employ a winding machine to neatly wind them together, creating a capacitor core package.
- (5) Impregnation: Soak the capacitor core with electrolyte to saturate the paper isolation layer and all parts of the corroded aluminum foil to ensure good contact between the oxide layer and the true cathode. This method requires the removal of gas from the core package and vacuum immersion of the electrolyte.
- (6) Assembly: To prevent evaporation or moisture absorption of the electrolyte, which can lead to deterioration, it is imperative to insert the capacitor core into a metal casing and securely seal it. Furthermore, to safeguard against the potential for electrolytic capacitor explosion due to excessive gas pressure during faults, a pressure relief device must be integrated.
- (7) Aging: Repair the oxide film that may be damaged during the manufacturing process, especially during cutting and assembly, by applying a DC voltage.
- (8) Inspection: After sealing, inspect the product for capacitance, leakage current, appearance, and performance as required, and then proceed with packaging.

2.2.2. Tantalum Electrolytic Capacitor

After aluminum electrolytic capacitors gained widespread use, issues such as limited lifespan and inadequate high-temperature resistance became apparent, prompting the development of tantalum electrolytic capacitors. These capacitors, similar to other electrolytic types, consist of an anode, electrolyte, and cathode. The cathode can be either solid or liquid, but currently, the majority of tantalum electrolytic capacitors available on the market are of the solid variety.

Solid tantalum electrolytic capacitors are composed exclusively of stable, inorganic, and nonvolatile materials devoid of any water or other liquids. This composition endows them with numerous advantages, including compact size, excellent temperature characteristics, the elimination of sealing requirements, and an extended service life [55,56]. However,

solid electrolytes have poor productivity and high costs, and the capacity achievement rate during use is generally poor [57].

Distinct from aluminum electrolytic capacitors, solid tantalum electrolytic capacitors employ tantalum powder sintered into porous tantalum blocks as the anode. The surface of these porous tantalum blocks is then oxidized to create an insulating medium composed of tantalum pentoxide [58]. The cathode, on the other hand, consists of manganese dioxide, which is in intimate contact with the tantalum pentoxide. The tantalum electrolytic capacitor is completed by drawing out the electrode. Notably, solid tantalum electrolytic capacitors are polarized capacitors, necessitating their use in a unipolar state; reverse polarity is strictly prohibited. The digital image and structure of this capacitor are illustrated in Figure 12.

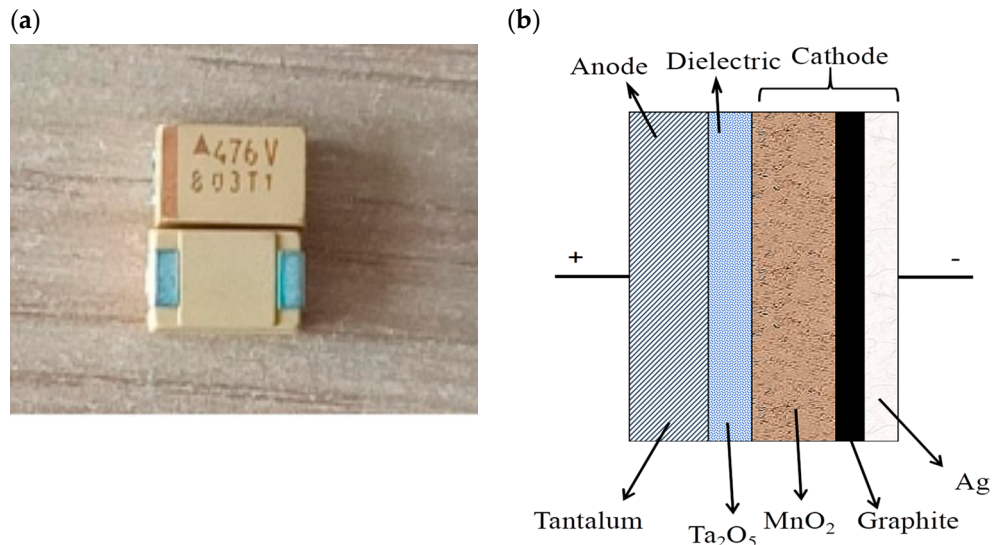


Figure 12. (a) Digital images of tantalum electrolytic capacitors. (b) Schematic diagram of tantalum electrolytic capacitor structure.

The production of solid tantalum electrolytic capacitors mainly involves the following steps (Figure 13) [31,59,60]:

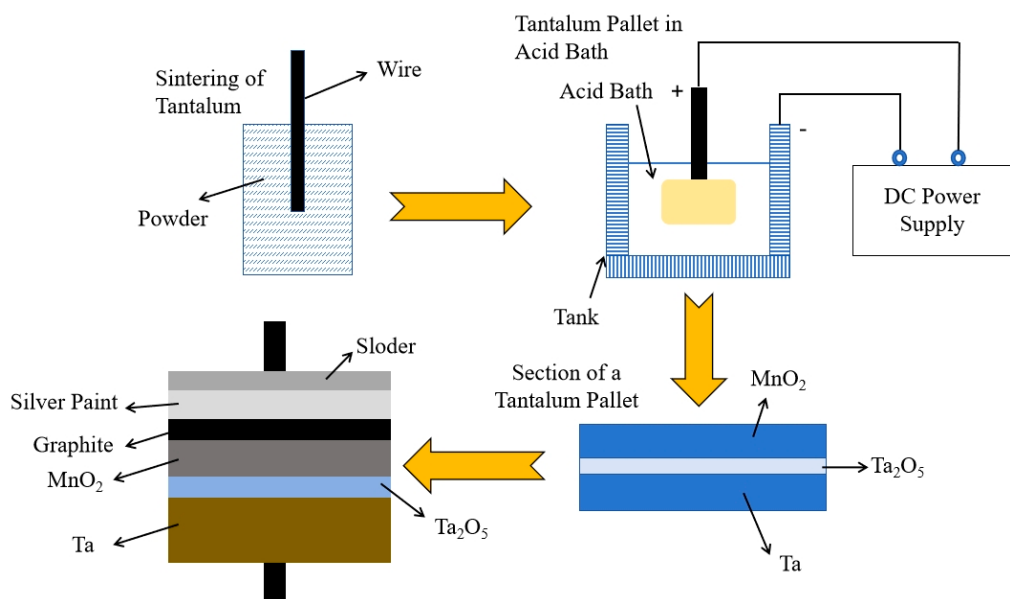


Figure 13. Fabrication process of solid electrolyte capacitor. Reproduced from Ref. [31] with permission.

- (1) The tantalum metal is crushed into a fine powder and thoroughly mixed with organic solvents. This mixture is then pressed into a desired shape under pressure, with tantalum leads embedded within. Subsequently, the assembly is sintered in a vacuum high-temperature environment, transforming it into a sponge-like structure. This process creates a highly porous metal anode, which significantly enhances its capacitance value. At the same time, it is truly integrated with the lead wire.
- (2) The sponge-like tantalum is submerged in a phosphoric acid solution for electrolysis. Through the process of oxidation, tantalum pentoxide is formed on its surface. This anode is then further coated with an insulating oxide layer, specifically tantalum pentoxide, serving as the dielectric layer. This comprehensive treatment process is referred to as anodizing.
- (3) Liquid manganese nitrate is added to the tantalum blocks, followed by thermally decomposing them in an environment containing water vapor and a catalyst. This process results in the production of manganese dioxide. Due to the excellent adsorption properties of manganese nitrate, the generated manganese dioxide is able to be fully adsorbed into the numerous tiny pores within the sponge-like tantalum block. Alternatively, if a solid polymer with a lower melting point is utilized, it can be melted and directly placed into the small pores.
- (4) Finally, silver powder and graphite are coated on the surface of manganese dioxide to reduce its equivalent resistance and enhance its conductivity. At the same time, external leads are added and packaged with epoxy resin.

In addition, there is another type of tantalum capacitor called a wet tantalum electrolytic capacitor, which uses a liquid electrolyte (usually sulfuric acid) instead of a solid electrolyte. The initial steps of anode production and dielectric deposition for wet tantalum electrolytic capacitors mirror those employed for solid tantalum capacitors. Subsequently, the dielectric-coated anode is submerged in a cage filled with the electrolyte solution. This cage, along with the electrolyte solution, collectively fulfills the role of the cathode in wet tantalum capacitors [31]. Wet tantalum electrolytic capacitors can be used at high temperatures and high ripple currents and are generally used in military and aerospace fields [61].

Although electrolytic capacitors share the self-healing ability with metallized thin film capacitors, the underlying mechanisms differ. In non-solid electrolytic capacitors, if the anodic oxide film sustains partial damage during operation or storage, the electrolyte serving as the cathode comes into play. Under the influence of the applied voltage, the non-solid electrolyte releases oxygen, which regenerates the oxide film at the damaged spot, thereby restoring its functionality. On the other hand, solid tantalum electrolytic capacitors may encounter cracks or metal impurities in the tantalum pentoxide film, resulting in an elevated leakage current. In this case, due to the high current density and temperature in the defective region, MnO_2 can locally transform into manganese oxides with high resistance, such as Mn_2O_3 and Mn_3O_4 , thereby isolating the breakdown point and preventing capacitor failure [62]. This process effectively repairs the defect, exhibiting the self-healing property of these capacitors.

2.3. Ceramic Capacitors

In ceramic capacitors, ceramic materials serve as dielectrics, while conductive metals function as electrodes. These capacitors are extensively employed in electronic devices because of their abundant raw materials, uncomplicated design, affordable price, and vast range of electrical capacity. Ceramic capacitors come in diverse types, primarily categorized as Class I and Class II, based on the characteristics of the dielectric materials employed [63]. Class I ceramic capacitors, commonly referred to as high-frequency ceramic capacitors, exhibit low dielectric loss, high insulation resistance, and a linear variation in dielectric constant with temperature. These capacitors are ideal for resonant circuits, filters, and temperature compensation. On the other hand, Class II ceramic capacitors, also known as low-frequency ceramic capacitors or ferroelectric ceramic capacitors, utilize ferroelectric

ceramics as their dielectric. They offer higher specific capacitance, non-linear capacitance changes with temperature, and increased losses. Therefore, they are commonly utilized for bypass or coupling applications in electronic devices [64]. In addition, according to their shape and structure, they can be divided into ceramic disk capacitors and multilayer ceramic capacitors (MLCCs).

Recently, research on ceramic capacitors has primarily focused on enhancing the performance of MLCC. Yong et al. [65] proposed a method of applying polydopamine (PDA) as a robust coating layer for MLCC. The barium titanate particles treated with PDA exhibited improved dispersion stability, preventing particle reagglomeration and contributing to the enhancement of the mechanical properties of MLCC. Lv et al. [66] developed a novel lead-free MLCC composed of $\text{NaNbO}_3-(\text{Bi}_{0.5}\text{Na}_{0.5})\text{TiO}_3-\text{Bi}(\text{Mg}_{0.5}\text{Hf}_{0.5})\text{O}_3$, which demonstrated exceptional performance, including a recoverable energy density of up to 12.65 J cm^{-3} and an energy efficiency of 88.5%.

2.3.1. Ceramic Disc Capacitors

Ceramic disc capacitors are constructed by applying silver contacts to both faces of a ceramic disc (shown in Figure 14a). Here, the ceramic disc serves as the dielectric material, while the silver coating on both sides functions as the electrodes of the capacitor. The leads, made of copper, are welded to the ceramic disc to establish electrical connections. Figure 14b shows actual images of ceramic disc capacitors. When its cross-section is placed under a scanning electron microscope, the observed images are shown in Figure 14c,d.

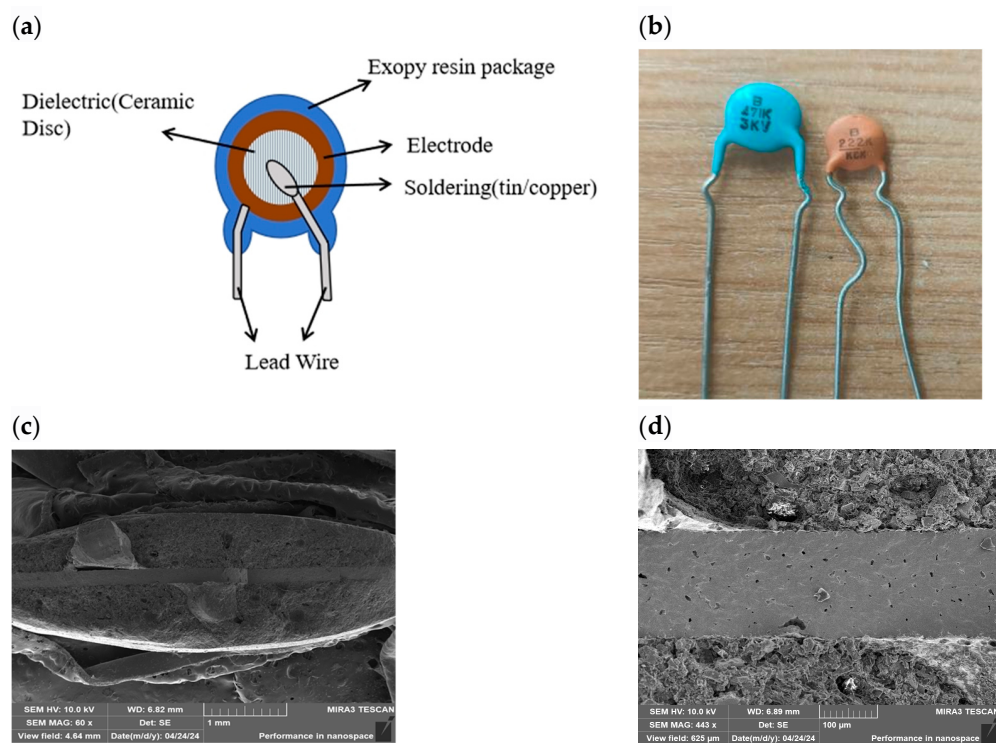


Figure 14. (a) Ceramic disc-type capacitor. (b) The actual images of ceramic disc capacitors. (c) The cross-section of the ceramic disc capacitor observed under a scanning electron microscope, which shows that the leads are bonded to the electrodes coated on both sides of the ceramic. (d) Enlarged cross-sectional view of a ceramic capacitor. In the middle is the ceramic dielectric, with electrodes coated on both sides and an outer layer of protective material.

Ceramic disc capacitors are extensively utilized in general electronic circuits due to their cost-effectiveness and ease of soldering. The capacitance of these capacitors is determined by the area of the ceramic disk or dielectric, as well as the spacing between the silver electrodes. For disc capacitors with lower capacitance, a single ceramic disc

coated with silver contacts is sufficient, while for high capacitance ceramic disc capacitors, multilayer ceramic discs are required [64]. The preparation of ceramic discs is similar to traditional ceramic processing. Initially, the dielectric powder undergoes ball milling to disaggregate it. Subsequently, an organic binder is added to prepare the powder for the forming process. After spray drying, the powder is fed into an automatic granulator to shape it into a raw disk. Next, two firing processes are carried out: the first to burn out the binder at a temperature below 550 °C, removing organic components, and the second sintering process at over 1000 °C to consolidate the ceramic particles into a solid body. Then, electrodes are applied to both sides of the disc using a paste containing metal particles (such as silver) and glass frit, followed by heat treatment. During this treatment, the glass material melts, ensuring strong adhesion of the metal electrode to the ceramic surface at a relatively low processing temperature. Finally, after attaching the leads to the electrodes, an epoxy or phenolic coating is applied to safeguard the ceramics from environmental contaminants [64].

2.3.2. Multilayer Ceramic Capacitor

The multilayer ceramic capacitor (MLCC) stands as a pivotal passive surface mount component in contemporary electronic devices. Its genesis dates back to the 1960s when American companies pioneered its successful development. Subsequently, Japanese companies like Murata, TDK, and Sunpower spearheaded its rapid industrialization and refinement. These companies continue to uphold their global supremacy in the MLCC industry, exemplified by their proficiency in manufacturing MLCCs that boast high reliability, precision, integration, and frequency, along with intelligence, low power consumption, immense capacity, miniaturization, and cost-effectiveness.

The MLCC is fabricated by stacking multiple layers of ceramic material interspersed with conductive electrodes [67,68]. Each layer of ceramic material sandwiches the electrodes, serving as the dielectric for the capacitor. These multilayer ceramic media and electrodes are interconnected through the terminal's surface, creating a compact and efficient structure. In other words, the MLCC is constructed by alternately layering ceramic dielectric membranes (commonly rutile titanium dioxide or barium titanate) with printed electrodes (inner electrodes) in a staggered configuration. This assembly is then consolidated into a ceramic chip through a single high-temperature sintering process. Subsequently, a metal layer (outer electrode) is applied to both ends of the chip, completing the manufacturing process. Its structure is shown in Figure 15a. The MLCC boasts not only the benefits of standard ceramic dielectric capacitors but also exhibits a range of exceptional characteristics. These include compact size, substantial capacity, high mechanical strength, excellent moisture resistance, outstanding high-frequency performance, and remarkable reliability [69,70]. Given its versatility and superior performance, the MLCC finds widespread application in various electronic information fields, encompassing mobile phones, computers, the military industry, aerospace, and beyond [71,72]. The packaging forms of MLCC mainly include wire-bonded and surface-mount types. The wire-bonded type was previously known as the monolithic capacitor (shown in Figure 15b). Its name originated from the fact that the ceramic dielectric body coated with metal electrodes is sintered with the electrodes into a single unit, resembling a stone block, hence the name "monolithic capacitor." Removing the leads from the monolithic capacitor results in the surface-mount packaging form (shown in Figure 15c). The observed images of the surface-mount type MLCC placed under a scanning electron microscope are shown in Figure 15d–g.

The production of surface-mount MLCC encompasses multiple processes, including the formation of ceramic dielectric films, the fabrication of inner electrodes, the creation of capacitor chips, sintering them into ceramics, the construction of outer electrodes, performance testing, and packaging, among others [64,73,74]. The specific process diagram is shown in Figure 16. Firstly, the dielectric powder is mixed with solvents, dispersants, binders, and plasticizers to form a homogeneous suspension. This slurry is then transferred to a casting machine, where a scraper evenly applies it onto a tape. The tape, coated

with the mixed slurry, is sent to a tape-casting machine where a doctor blade precisely scrapes the slurry onto it. The resulting wet sheet is subsequently dried, transforming into a flexible tape. Next, an electrode paste is applied to the tape in a designed pattern through screen printing. During the lamination process, the printed tapes are stacked layer by layer with precision alignment. After cutting and separation, each green MLCC undergoes high-temperature sintering to eliminate the adhesive and organic matter. This sintering process also solidifies the layers of dielectric tape and electrodes, creating a dense structure. Additionally, the sintered ceramic is chamfered to fully expose the inner electrodes.

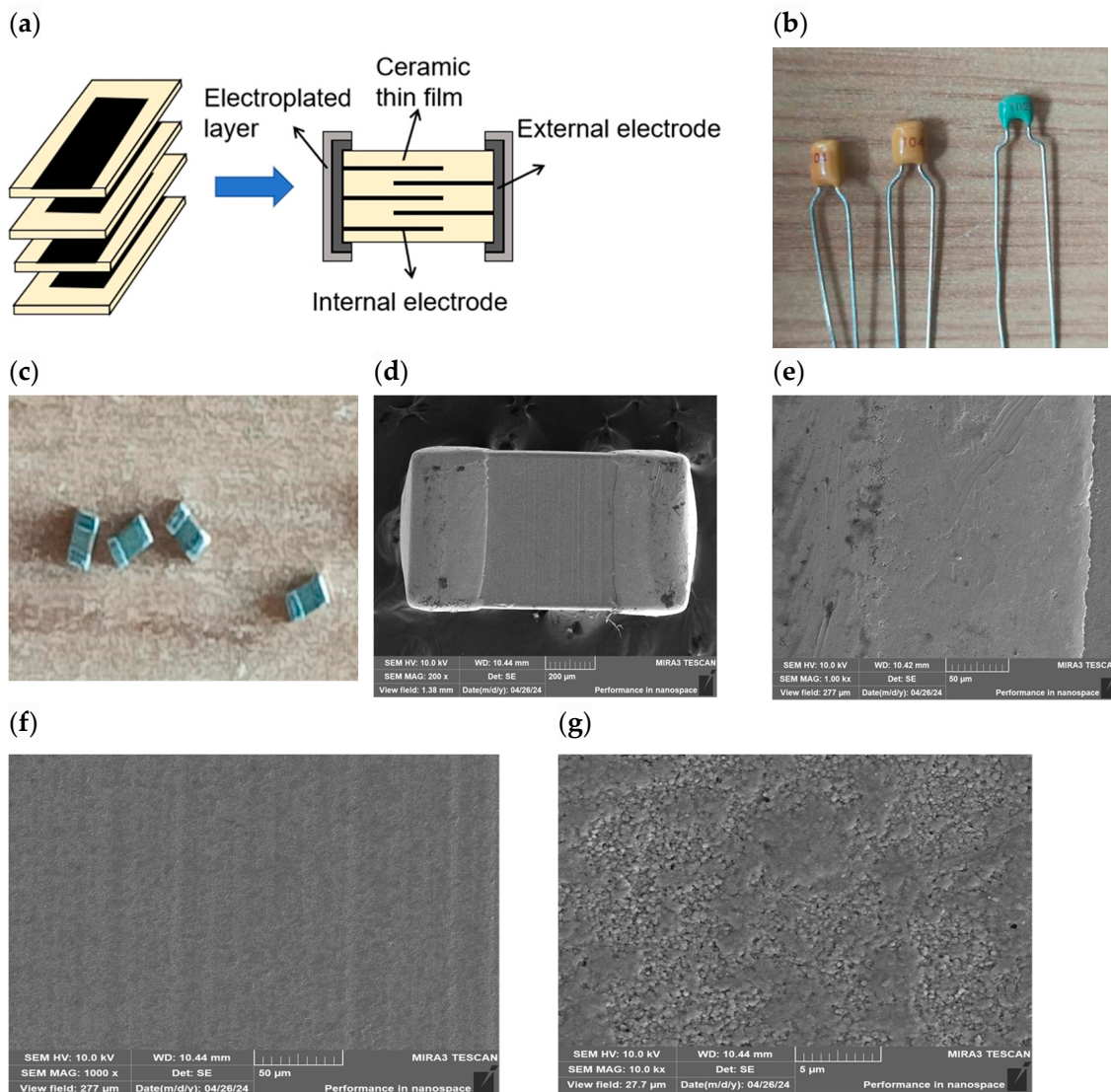


Figure 15. (a) Schematic diagram of MLCC structure. (b) The actual image of the monolithic ceramic capacitor. (c) The actual image of the surface-mount packaging form. (d) The overall structural diagram of the surface-mount type MLCC under a scanning electron microscope, which shows that MLCC is constructed by stacking ceramic dielectric sheets with printed electrodes in a staggered manner to form a layered structure. (e) The external electrode of MLCC, which is composed of an electroplated metal layer. (f) The internal electrode of MLCC, which is composed of metallic materials. (g) The dielectric of MLCC, which is composed of ceramic materials.

To form the outer electrode, electrode paste is applied to the exposed inner electrodes, connecting the inner electrodes on the same side. Notably, the surface-mount MLCC achieves electrical connection through three consecutive layers of termination electrodes [75]. The first layer, in contact with the inner electrode, is copper. Nickel serves as an

intermediate layer, electroplated onto the copper, acting as a thermal barrier to safeguard the capacitor during welding. Finally, a layer of tin is applied to the nickel to enhance solderability. After the completion of outer electrode production, rigorous performance testing and packaging procedures are conducted to eliminate any defective products.

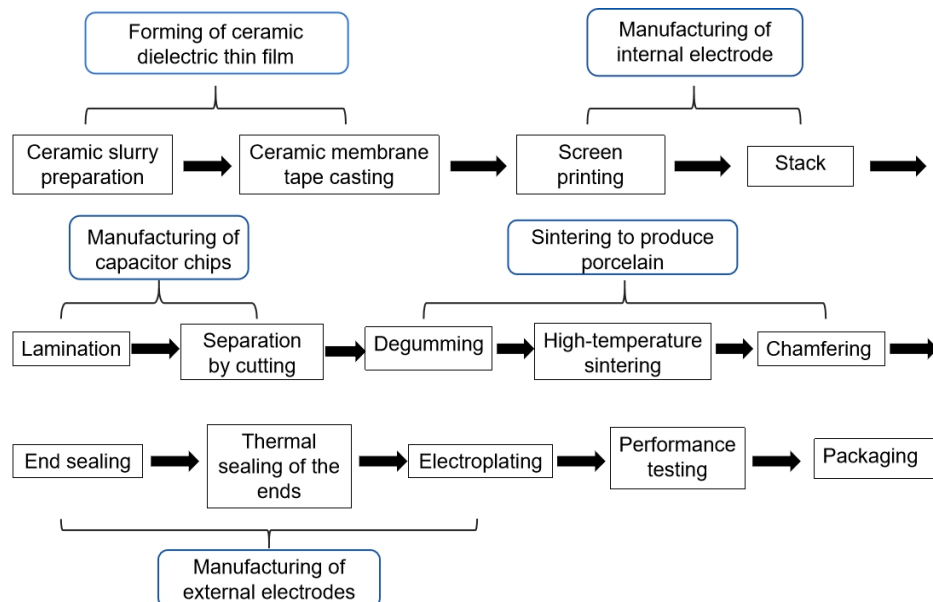


Figure 16. MLCC manufacturing process flowchart.

2.3.3. Others

In recent years, researchers have been paying attention to a new type of capacitor, namely, the multilayer polymer capacitor (MLPC), which has a similar design as MLCC and exhibits extremely high application value. Different from traditional solid capacitors, MLPC adopts a unique chip-type multilayer structure. Its production process is elaborately designed. Firstly, the aluminum foil is etched to form a porous oxide layer, and then a conductive polymer is deposited on the oxide layer as the cathode. After that, these treated aluminum foils are stacked into a multilayer structure, and then carbon paste is applied on them to form a carbon coating, followed by the application of silver paste to form a silver coating. Finally, the entire structure is completely sealed and fixed with epoxy resin, which can effectively protect its internal structure and prevent local overheating.

Compared with MLCC, MLPC has a higher capacity, which can significantly reduce the number of capacitors required in applications, thus reducing the overall cost. Moreover, MLPC exhibits excellent performance in high and low-temperature environments, overcoming the cracking issues that MLCC may encounter due to temperature or mechanical shock, thereby improving the reliability and stability of the product. Compared with solid tantalum capacitors, MLPC has a lower equivalent series resistance and higher safety. Currently, the conductive polymer of MLPC is mainly based on poly(3,4-ethylenedioxothiophene) (PEDOT), and the deposition technology often adopts *in situ* polymerization. The development of new conductive polymers and the optimization of polymer deposition technology have become research hotspots in recent years.

3. Electrochemical Capacitor

Electrochemical capacitors, commonly referred to as supercapacitors (SCs), possess remarkable charge and discharge efficiency, an outstanding cycle life, and exceptional power performance while being capable of operating across a broad temperature spectrum [76,77]. In comparison to batteries, supercapacitors exhibit a superior power density and the ability to rapidly store or discharge energy [78]. Nevertheless, their energy density is lower due to the constraints associated with electrode surface charge storage. When compared to

traditional capacitors, they possess a lower power density but a higher energy density [79]. Supercapacitors can serve as rapid starting power sources for electric vehicles, as well as balancing power supplies for lifting equipment. Furthermore, they can be utilized as traction energy sources for hybrid electric vehicles, internal combustion engines, and trackless vehicles [80–82].

The history of supercapacitors can be traced back to 1853. In 1853, Helmholtz pioneered the exploration of electrical storage mechanisms within capacitors and introduced the concept of the double-layer model in the context of colloidal suspension research. In 1957, Becker filed the first patent for an electrochemical capacitor, which incorporated porous carbon electrodes immersed in an H_2SO_4 solution [83]. Advancing further, in 1971, Trasatti and his colleagues reported for the first time on the charge storage behavior of ruthenium oxide films in sulfuric acid, revealing the pseudocapacitance phenomenon in transition metal oxides. Subsequently, Shirakawa et al. garnered attention for the pseudocapacitive charge storage properties they developed in conductive polymer materials, thus propelling the interest in pseudocapacitors [84]. In 1978, NEC Corporation of Japan commercialized electrochemical capacitors, branding them “supercapacitors.” A decade and a half later, in 1989, the U.S. Department of Energy initiated long-term research support for high-energy-density supercapacitors intended for use in electric drive systems as part of their electric and hybrid vehicle initiatives. Presently, leading global supercapacitor companies such as Maxwell (USA), Nesscap (South Korea), ELTON (Russia), and Nippon Chemicon (Japan) have developed and offered a diverse range of supercapacitors for commercial applications [85].

In recent years, researchers have proposed numerous approaches to improve the performance of supercapacitors. Zan et al. [86] employed a self-template biomimetic method to synthesize a novel mesoporous Ni(OH)_2 structure, which comprises house-of-cards-like cubic nanocages assembled from monolayer Ni(OH)_2 coupled with an exceptionally large interlayer spacing of approximately 1 nm. Tests have shown that it provides a specific capacity close to 100% of the theoretical value and exhibits an excellent cycling performance of over 10,000 cycles. Shwetha et al. [87] synthesized Co_3O_4 nanoparticles using a mixture of cobalt nitrate and ascorbic acid. Electrochemical data indicate that the Co_3O_4 nanoparticles exhibit good capacitive behavior, with the highest electrochemical performance observed when the cobalt nitrate/ascorbic acid ratio equals 1. Specifically, these nanoparticles deliver a specific capacitance of 166 F g^{-1} at a current density of 0.5 A g^{-1} and retain 90% of their capacitance after 5000 cycles. Luo et al. [88] reported a method for synthesizing heterogeneous $\text{Ni}_3\text{N}-\text{Co}_2\text{N}_{0.67}$ /nitrogen-doped carbon ($\text{Ni}_3\text{N}-\text{Co}_2\text{N}_{0.67}/\text{NC}$) hollow nanoflowers by pyrolyzing a NiCo-TEOA (triethanolamine) complex precursor and employing urea as a nitrogen source. The assembled $\text{Ni}_3\text{N}-\text{Co}_2\text{N}_{0.67}/\text{NC}/\text{AC}$ battery achieves a peak energy density of 32.4 W h kg^{-1} at a power density of 851.3 W kg^{-1} . Wang et al. [89] proposed an effective method for activating Ni-Co oxide nanosheet arrays (NiCoO NSAs) grown on carbon fiber cloths. The resulting ac-NiCoO NSA exhibits a high specific capacity (206.5 mAh g^{-1} at 0.5 A g^{-1}). The assembled capacitor demonstrates high energy density (45.4 Wh kg^{-1}), high power density (17.3 kW kg^{-1}), and ultra-long cycling stability, with a retention rate of 77.4% after 20,000 cycles (20 A g^{-1}).

Furthermore, in recent years, flexible supercapacitors, which exhibit both bendability and stretchability coupled with their high electrochemical performance retention, have garnered extensive and intensive research attention. Song et al. [90] have developed a self-wrinkled polyaniline (PANI)-based composite hydrogel (SPCH), featuring an electrolyte hydrogel and PANI composite hydrogel as its core and shell, respectively, through a stretching, low-temperature polymerization/release strategy. This SPCH exhibits remarkable stretchability (approximately 970%) and high fatigue resistance. Remarkably, upon cutting and reconnecting the edges, it can directly function as an intrinsically stretchable all-solid-state supercapacitor (A-SC), maintaining highly stable output with a capacitance retention rate of 92% even after 1000 stretching and releasing cycles at 100% strain. Huai et al. [91] synthesized cobalt-doped NiMoO_4 nanosheets via a hydrothermal method, which exhib-

ited a specific capacitance of 906 C g^{-1} at a current density of 1 A g^{-1} . The assembled flexible supercapacitor delivered an energy density of 64 Wh kg^{-1} at a power density of 2880 W kg^{-1} . Notably, the device retained 78% of its initial capacitance after 10,000 cycles. Liu et al. [92] prepared graphene/MnO₂ composites by growing MnO₂ nanosheets on single-layer graphene via a water bath method and introducing two-dimensional black phosphorus during the pulping process. These composites were used to fabricate micro-supercapacitors that can be integrated with flexible film pressure sensors, holding promise for wearable electronic devices. Zhu et al. [93] provided an overview of solid-state flexible supercapacitors, reviewed the current research status of vanadium-based electrode materials in solid-state flexible SC, and proposed strategies to address the challenges associated with these materials. Wang et al. [94] introduced a fully biomass-based colloidal gel composed of a mononuclear anthraquinone derivative and porous lignin-based graphene oxide fabricated through a self-assembly process. This gel was successfully used to produce biomass-based flexible micro-supercapacitors via screen printing. Upon testing, these capacitors demonstrated significant areal capacitance (43.6 mF cm^{-2}), energy and power densities ($6.1 \mu\text{Wh cm}^{-2}$ and $50 \mu\text{W cm}^{-2}$, respectively), and cyclic stability (>10,000 cycles).

In recent years, numerous review articles have outlined the research progress in supercapacitor electrode materials and electrolytes. Li et al. [95] comprehensively summarized the research advancements in nickel-based composites for supercapacitors, encompassing the properties of novel materials, preparation methods, and application potentials, offering insights into the research prospects and future trends of nickel-based composites. Troschke et al. [96] introduced the general chemical properties of Schiff bases and reviewed several nanomaterials and their carbonized derivatives obtained through Schiff-base formation, along with an outlook on the major obstacles and future prospects in this research field. Shi et al. [97] overviewed the research progress in redox electrolyte-enhanced carbon-based supercapacitors, analyzing the causes of self-discharge and corresponding suppression strategies from aspects such as separator modification, electrolyte formulation, and electrode design while outlining their development prospects. Wu et al. [98] reviewed the research progress of various spatially dimensional carbon materials in recent years, discussing their advantages and disadvantages as supercapacitor electrode materials, examining the key factors influencing their electrochemical performance, and proposing new development trends for carbon materials. Kong et al. [99] introduced the concept of superstructured carbons with customized functionality, comprehensively outlining their designs tailored to different energy storage mechanisms and prospectively pointing out potential challenges in their future development. Although these reviews have thoroughly explored supercapacitor electrode materials or electrolytes, a comprehensive overview of their structures and energy storage principles remains lacking. Thus, the present review focuses on elucidating the classification, fine structures, and unique energy storage mechanisms of supercapacitors, aiming to provide readers with a more complete and in-depth understanding of the framework.

The structure of a supercapacitor comprises four main components: two electrodes, an electrolyte, a separator, and current collectors. The function of current collectors is to collect the current generated by the active material in the capacitor and facilitate the formation of a larger current for external output. Typically, copper foil is used as the current collector for the negative electrode, while aluminum foil is employed for the positive electrode. Depending on the energy storage principle, SC can be categorized into three types, namely electrochemical double-layer capacitors (EDLCs), pseudocapacitors, and hybrid capacitors, as illustrated in Figure 17 [100,101]. Their respective energy storage mechanisms are based on non-Faradaic, Faradaic, and a blend of both processes [102]. In the non-Faradaic process, charges are distributed across the surface through physical means without the formation or breakdown of chemical bonds [103]. Conversely, the Faradaic process involves the transfer of charges between electrodes and electrolytes. Double-layer capacitors store energy through non-Faradaic reactions, commonly utilizing carbon-based materials with a

high surface area and porosity as electrode materials. On the other hand, pseudocapacitors store energy through Faradaic reactions, typically employing transition metal oxides (like RuO_x) and conductive polymers (such as polyaniline) as electrode materials [104]. In hybrid capacitors, both Faradaic and non-Faradaic reactions occur for energy storage, combining the benefits of EDLC and pseudocapacitors [105].

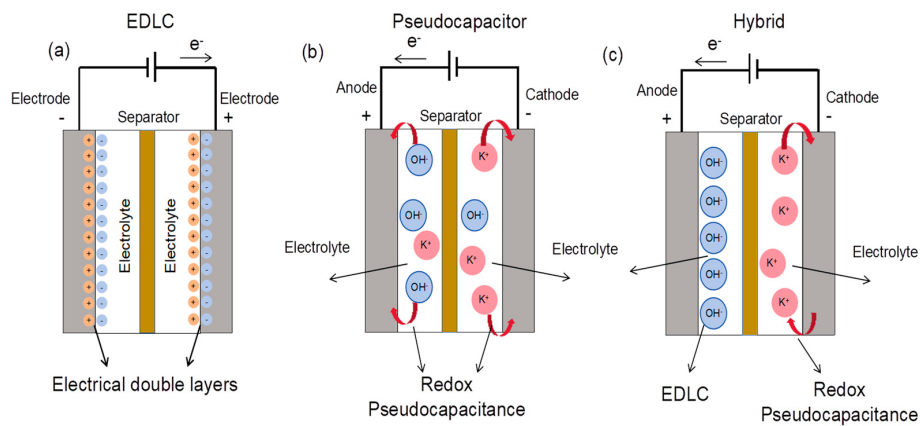


Figure 17. Types of supercapacitors. (a) EDLC. (b) Pseudocapacitors. (c) Hybrid supercapacitors. Reproduced from Ref. [106] with permission.

Supercapacitors and electrolytic capacitors seem superficially similar due to their shared electrolyte component. Both aim to enhance capacitance by increasing electrode area and reducing electrode distance. However, a deeper exploration reveals significant differences. The electrolyte in aluminum electrolytic capacitors is the actual cathode, while the electrolyte in supercapacitors is the dielectric, with porous activated carbon comprising the actual electrode. Traditional electrolytic capacitors utilize valve metal as the electrode and its oxide as the dielectric, resulting in polarity and intolerance to reverse voltage. Conversely, supercapacitors exhibit identical electrode structures, classifying them as non-polar capacitors.

3.1. Electrochemical Double-Layer Capacitors

The concept of the double layer was originally introduced and formulated by von Helmholtz in the 19th century, with subsequent modifications and enhancements made by Gouy, Chapman, and Stern [107]. EDLC comprises two carbon-based electrodes, a separator, and an electrolyte [108]. Charge storage is achieved by the formation of a double layer at the interface between the electrode and the electrolyte [109]. The physical image and the dismantled structural diagram of EDLC are shown in Figure 18. During the operation of an EDLC, charge accumulation occurs through a non-Faradaic process, meaning that there is no ion exchange between the electrode material and the electrolyte solution, and electrons do not transfer across the electrode interface [110]. When charging, electrons are driven by an external electric field to move from the positive electrode to the negative electrode through an external circuit, resulting in the formation of a layer of charge electrons on the surface lattice structure of the electrode material [110]. In electrolytes, anions are attracted toward the positive electrode, while cations migrate toward the negative electrode. These oppositely charged ions migrate toward the respective electrodes and accumulate on their surfaces, creating a double layer. Upon removal of the external electric field, the double layer persists, stabilizing the voltage due to the attractive forces between the opposing charges [80]. During discharge, the process reverses. The charged ions adsorbed on the electrode migrate in a directional manner, generating a current in the external circuit until the electrolyte returns to its electrically neutral state. This charge storage mechanism is fully reversible, and since it lacks chemical reactions, the electrode structure of the EDLC remains virtually unchanged. This attribute confers EDLC capacitors with a prolonged cycle life and exceptional power density [109,111].

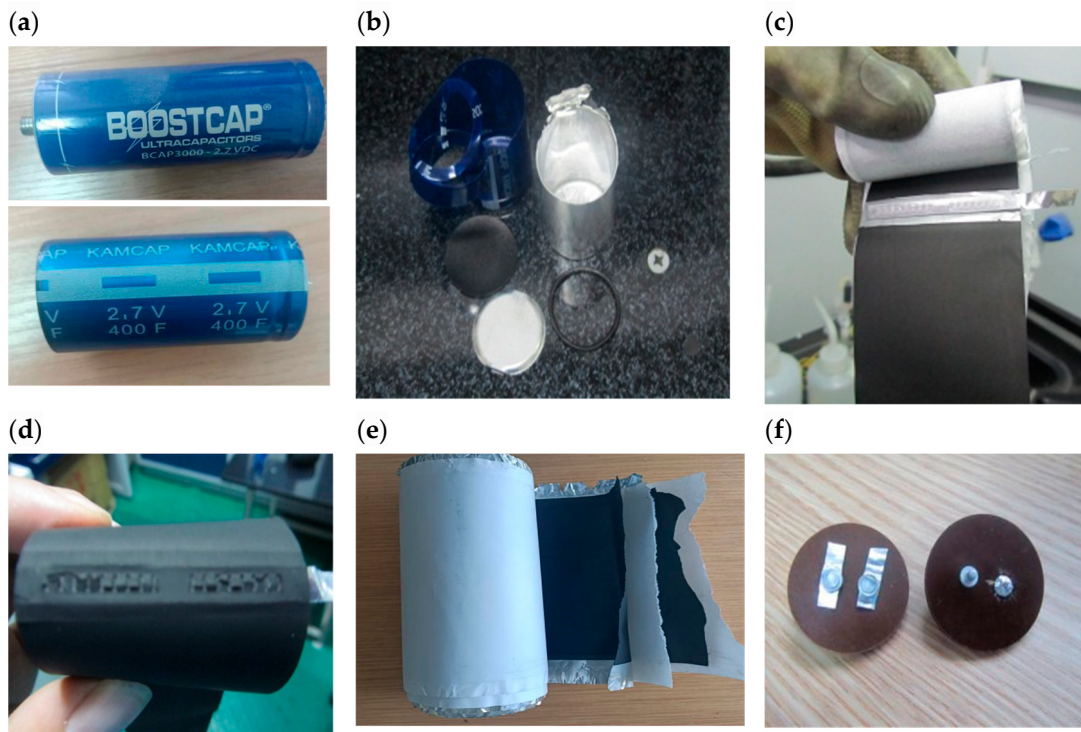


Figure 18. (a) The physical image of an EDLC. (b) The bottom gasket, insulating sheet, top sealing ring, outer aluminum case, and packaging plastic film of the EDLC. (c) Lead-out welding spot. (d) The back of the welding spot. (e) The overall structure of the EDLC. (f) Top rivet.

The electrode materials of EDLC commonly consist of carbon-based substances, encompassing activated carbon (AC) [112–114], carbon nanotubes (CNTs) [115], graphene [116,117], and various other carbon-based composite materials. These materials are deemed suitable for double-layer capacitors, attributed to their expansive specific surface area, robust thermal and electrochemical stability, and superior conductivity [107]. Currently, research in the field of EDLC is focused on two major directions: optimizing the performance of existing electrode materials and developing new materials. Fu et al. [118] obtained nitrogen and sulfur dual-doped activated carbon with a hierarchical pore structure by directly carbonizing/activating polymer-based monolithic materials. The EDLC assembled with this material exhibits favorable energy density and power density in a $6 \text{ mol}\cdot\text{L}^{-1}$ KOH aqueous electrolyte. Lv et al. [119] utilized dopamine and copper chloride precursors to form carbon flocculates embedded with ultrafine copper nanoparticles on carbon cloth through pyrolysis and electrochemical oxidation reactions. The results indicated that the obtained electrode possessed a large surface area of $55.5 \text{ m}^2\cdot\text{g}^{-1}$ and a high conductivity of $48.7 \text{ S}\cdot\text{mm}^{-1}$. When the prepared material was applied in an EDLC, the EDLC exhibited outstanding performance with a power density as high as $179 \text{ mW}\cdot\text{cm}^{-3}$ and an energy density reaching $23 \text{ mWh}\cdot\text{cm}^{-3}$, demonstrating promising application prospects. Yoo et al. [120] successfully prepared cost-effective carbon xerogels with large surface areas by substituting phenol for resorcinol and controlling the amount of catalyst, further confirming their excellent electrochemical performance as active materials for EDLC electrodes.

The performance of EDLC is also influenced by the compatibility between the pore size of the electrode material and the size of the electrolyte ions, as well as the ionic mobility. Consequently, the performance of EDLC can be altered by utilizing diverse electrolytes, including aqueous and organic electrolytes. Although aqueous electrolytes offer lower series resistance compared with organic electrolytes, their narrower potential window range restricts the energy density of EDLC [121]. During the production process, it is crucial to select an electrolyte solution that suitably adapts to the pore size of the electrode material.

3.2. Pseudocapacitors

In contrast to EDLC, a pseudocapacitor exhibits charge transfer at the electrode-electrolyte interface, enabling energy storage through a rapid and reversible Faradaic reaction. This mechanism enhances the energy density within the electrode [122]. Generally speaking, pseudocapacitance can be divided into three different types based on its reaction mechanism, including redox pseudocapacitance, under potential deposition (adsorption) pseudocapacitance, and intercalation pseudocapacitance [123]. The schematic diagrams of the three processes are shown in Figure 19.

3.2.1. Redox Pseudocapacitance

Redox pseudocapacitance (Figure 19a) is the most prevalent form of pseudocapacitance. Its working principle involves the electrochemical adsorption of active ions in the electrolyte onto or near the electrode surface when a potential is applied [124]. Simultaneously, the electrode material undergoes a rapid and reversible oxidation-reduction reaction, generating charges and facilitating Faraday currents to flow through the supercapacitor (Figure 19a) [125].

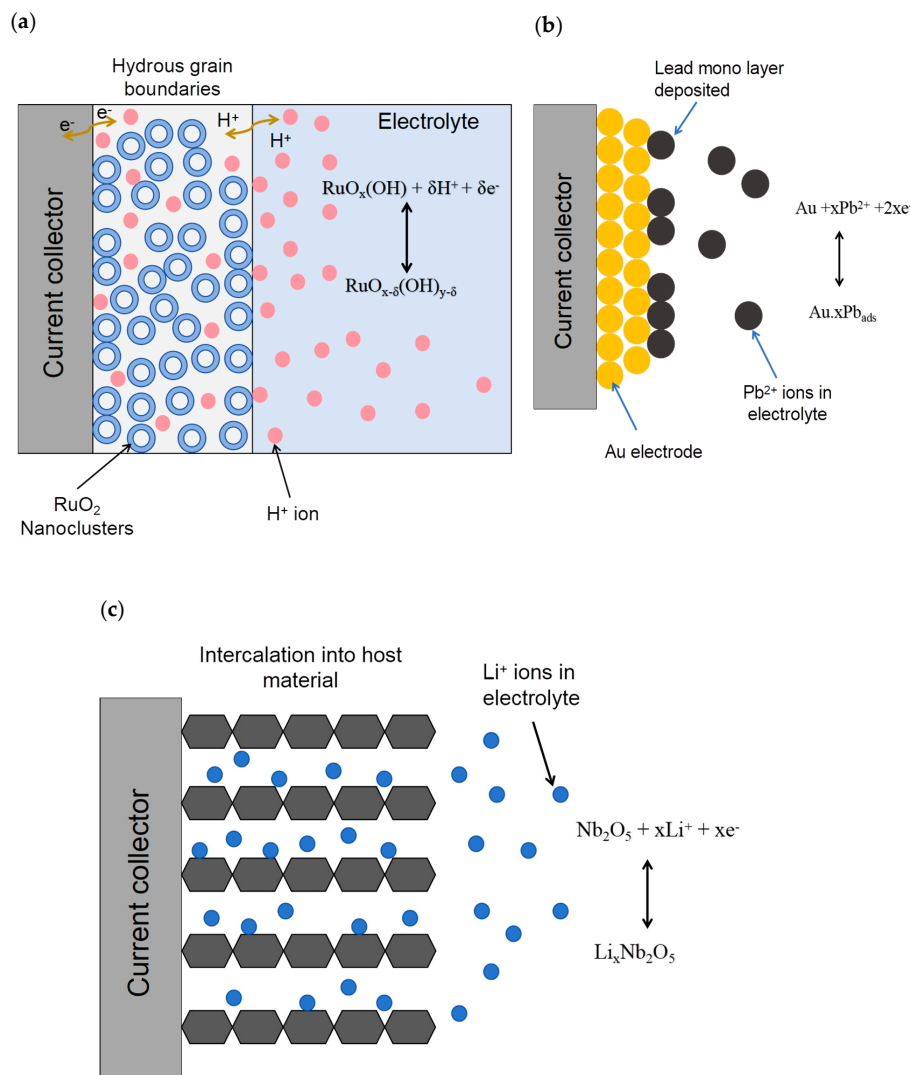


Figure 19. The schematic diagrams of pseudocapacitance. (a) A redox pseudocapacitance in RuO_2 schematics. (b) Underpotential deposition pseudocapacitance, Pb coating on Au electrode. (c) Intercalation pseudocapacitance, lithium ions embedded in the lattice of niobium oxide. Reproduced from Ref. [125] with permission.

3.2.2. Underpotential Deposition Pseudocapacitance

Underpotential deposition pseudocapacitance (Figure 19b), alternatively known as adsorption pseudocapacitance, occurs when an external potential is applied. This process involves the surface adsorption and reduction of metal ions, resulting in the deposition of a monolayer on the metal surface. This deposition causes a minor change in potential relative to its equilibrium potential. An example of underpotential deposition pseudocapacitance is the adsorption of lead onto the surface of an Au electrode (Figure 19b) [126].

3.2.3. Intercalation Pseudocapacitance

The principle of intercalated pseudocapacitors (Figure 19c) involves the embedding of ions from the electrolyte into the layered or tunnel-like structure of redox-active materials. This embedding process triggers rapid charge transfer, which occurs without altering the crystal structure of the electrode material [125]. One example is the insertion of lithium ions into the lattice of niobium oxide (Figure 19c) [127].

Pseudocapacitors possess distinct electrochemical characteristics, allowing for high charge storage capacity and a boost in energy density through efficient charge transfer channels [128]. Typically, pseudocapacitors exhibit superior specific capacitance and energy density when compared to EDLCs [129]. However, redox reactions, particularly those occurring on the electrode surface, can alter the bulk phase or electrolyte composition of the electrode material. Consequently, over extended charging and discharging cycles, materials are prone to fatigue damage, resulting in a shorter cycling life [80]. While their lifespan is still longer than that of batteries, it falls short of that of double-layer capacitors.

During the early stages of pseudocapacitive electrode research, researchers primarily focused on transition metal oxides (TMOs) [130]. Nevertheless, their practical applications have been unsatisfactory due to low conductivity and relatively limited charge storage capacity, thus limiting their widespread use in pseudocapacitive electrodes. Currently, electrode materials for pseudocapacitors that are widely studied include carbon materials doped with heteroatoms (such as N, P, S) [131], transition metal oxides/hydroxides (like MnO_2 , NiOOH) [132,133], two-dimensional transition metal carbides, and nitrides (MXene) [134]. Compared with pure carbon materials, carbon materials doped with heteroatoms possess characteristics such as low cost and excellent electrochemical performance. Commonly, N atoms, P atoms, and others are selected for doping. For instance, Cao et al. [135] prepared nitrogen-doped biomass-derived hierarchical porous carbon materials (HPC) using different nitrogen-containing compounds (NH_4Cl , $(\text{NH}_4)_2\text{CO}_3$, and urea) simultaneously as activators and dopants. When the three materials were used in pseudocapacitors, the pseudocapacitor based on HPC-urea exhibited the highest specific capacitance ($300 \text{ F}\cdot\text{g}^{-1}$ at $1 \text{ A}\cdot\text{g}^{-1}$) and energy density ($14.3 \text{ Wh}\cdot\text{kg}^{-1}$). As a transition metal oxide, MnO_2 boasts low cost and superior electrochemical performance, achieving a specific capacitance as high as $1100 \text{ F}\cdot\text{g}^{-1}$ within a potential window of 1.0 V . In recent years, MnO_2 has emerged as a research hotspot in the field of pseudocapacitive materials. The reversible transformation between MnO_2 and MnOONa in sodium sulfate electrolyte is the primary reason for the pseudocapacitive behavior exhibited by MnO_2 electrodes [136]. Currently, research on MnO_2 primarily focuses on enhancing its specific capacitance. For instance, Zhou et al. [137] successfully synthesized mesoporous manganese dioxide with a semicrystalline spinodal structure using mesoporous silica KIT-6 as a robust hard template. Within the potential range of -0.1 V to 0.55 V , this material exhibited stable and reversible electrochemical behavior, achieving an excellent capacitance performance of $220 \text{ F}\cdot\text{g}^{-1}$. Nayak et al. [138] obtained mesoporous manganese dioxide with an average pore diameter of $2\text{--}20 \text{ nm}$ from potassium permanganate through a sonochemical method using triblock copolymers as soft templates. These materials possess a high specific capacitance of $265 \text{ F}\cdot\text{g}^{-1}$. MXene is a novel class of two-dimensional transition metal carbides, carbonitrides, or nitrides. Its interlayer structure is flexible, allowing various ions to be inserted between MXene sheets. Additionally, due to its abundant interlayer ion diffusion pathways and ion storage sites, combined with the conductive carbide/nitride core within the mate-

rial, MXene has emerged as an important candidate for pseudocapacitive energy storage materials [139]. Cao et al. [140] have developed highly stretchable micro-pseudocapacitor electrodes composed of MXene nanosheets and *in situ* reconstructed silver nanoparticles (Ag-NP-MXene). These electrodes exhibit high energy density, a stable operating voltage of approximately 1 V, and rapid charging capabilities. Kim et al. [141] immersed carbon nanofibers (CNFs) into a colloidal solution of MXene (Ti_3C_2) to form a composite material through a dip-coating process. Subsequently, they constructed a three-electrode system using an aqueous solution of 1 M sodium sulfate as the electrolyte. Experimental results showed that this MXene-coated CNF exhibited remarkable performance, achieving a maximum specific capacitance of $514 \text{ F}\cdot\text{g}^{-1}$ at a current density of $0.5 \text{ A}\cdot\text{g}^{-1}$. Additionally, the energy density and power density reached $71.4 \text{ Wh}\cdot\text{kg}^{-1}$ at $0.5 \text{ A}\cdot\text{g}^{-1}$ and $2.3 \text{ kW}\cdot\text{kg}^{-1}$ at $5 \text{ A}\cdot\text{g}^{-1}$, respectively.

3.3. Hybrid Capacitors

As implied by its name, a hybrid capacitor is essentially a type of supercapacitor that consists of two electrode parts and a separator. The electrodes of a hybrid capacitor can be made from dissimilar materials, and the separator typically has a microporous structure. The diversity in hybrid capacitors is achieved through the combination of various redox and EDLC materials. The storage mechanism of hybrid supercapacitors integrates the principles of both EDLC and pseudocapacitors. This unique combination results in a significantly higher capacitance, often reaching levels two to three times greater than those of traditional capacitors, standalone EDLCs, or pseudocapacitors. Additionally, it exhibits a higher working potential, further enhancing its overall performance [142]. The electrodes of hybrid supercapacitors are usually asymmetric, with one electrode being a carbon electrode that charges and discharges based on the double-layer capacitance process and the other electrode being a pseudocapacitive electrode material or battery electrode material that undergoes Faradaic redox reactions during charging and discharging.

The positive electrode of a hybrid capacitor is a crucial component that supports its high-current discharge and high-power density capabilities. Carbon-based materials, known for their high electrical conductivity and large specific surface area, are commonly used as positive materials in hybrid capacitors. The reaction mechanism of carbon-based positive materials is primarily based on the electric double-layer principle, where energy is stored and released through the adsorption and desorption of ions from the electrolyte onto the surface of the carbon electrode. Common carbon-based positive materials include activated carbon and graphene. Activated carbon features a porous structure, a large specific surface area (approximately $1000\text{--}1500 \text{ m}^2\cdot\text{g}^{-1}$), and strong adsorption capabilities [143]. However, its relatively low specific capacity (around $40\text{--}80 \text{ mAh}\cdot\text{g}^{-1}$) and electrical conductivity (approximately $1\text{--}5 \text{ S}\cdot\text{cm}^{-1}$) limit its applications to some extent. Currently, research on activated carbon materials focuses on optimizing their porous structure, morphology control, and surface modification to achieve higher specific capacitance. For example, Lu et al. [144] utilized corn stalks to prepare mesoporous activated carbon for use in high-performance supercapacitors. The activated carbon based on corn stalks exhibited a high specific capacitance of $188 \text{ F}\cdot\text{g}^{-1}$ at a current density of $1 \text{ A}\cdot\text{g}^{-1}$ in both organic and ionic liquid electrolytes. Piao et al. [145] reported an activated multi-hierarchical mesoporous carbon (MHPC). When tested in a three-electrode system using a 6 M KOH aqueous solution at a current density of $1 \text{ A}\cdot\text{g}^{-1}$, the assembled supercapacitor with the MHPC electrode achieved a specific capacitance of $318 \text{ F}\cdot\text{g}^{-1}$. Graphene is a two-dimensional monolayer material composed of carbon atoms arranged in a honeycomb lattice. It possesses a theoretical specific surface area of $2360 \text{ m}^2\cdot\text{g}^{-1}$, a theoretical specific capacitance of $550 \text{ F}\cdot\text{g}^{-1}$, and high electrical conductivity (approximately $50\text{--}150 \text{ S}\cdot\text{cm}^{-1}$). However, irreversible stacking tends to occur between graphene sheets, reducing their surface area [113]. Currently, researchers have employed various methods to address the aforementioned issues. For instance, Gao et al. [146] synthesized a three-dimensional oriented graphene framework that resembles paper but possesses a directed surface, macropores, and interconnected

parts through ordered assembly guided by hard templates. This framework exhibits a high specific surface area of up to $402.5 \text{ m}^2 \cdot \text{g}^{-1}$ and excellent mechanical flexibility, making it suitable for use as an electrode in hybrid capacitors. Yan et al. [147] prepared hollow graphene nanospheres through a combination of template separation, microwave heating, and graphitization of carbon layers. The synthesized graphene exhibits a specific surface area of $2794 \text{ m}^2 \cdot \text{g}^{-1}$, a capacitance exceeding $529 \text{ F} \cdot \text{g}^{-1}$ at a current density of $1 \text{ A} \cdot \text{g}^{-1}$, and a capacitance retention rate of 62.5% during continuous power supply.

For the negative electrode of hybrid capacitors, materials with rapid charge-discharge capabilities are often employed to compensate for the kinetic differences between the positive and negative electrodes. Transition metal oxides, with their high theoretical specific capacities, abundant sources, and low costs, are commonly used as negative electrode materials in hybrid capacitors. The reaction mechanism of transition metal oxide negative electrode materials is primarily based on Faraday redox reactions. When the hybrid capacitor is charged, ions in the electrolyte (such as sodium ions, lithium ions, etc.) diffuse to the surface of the transition metal oxide negative electrode material and undergo electrochemical reactions with it, storing charge. During this process, one or more redox pairs form on the surface of the transition metal oxide, which can reversibly convert during charging and discharging, thereby enabling the storage and release of charge. Common transition metal oxide materials include MnO and Co_3O_4 . When MnO is used as a negative electrode material, its theoretical capacity ratio can reach $756 \text{ mAh} \cdot \text{g}^{-1}$, but pure MnO has poor electronic conductivity (approximately $10^{-8}\text{--}10^{-6} \text{ S} \cdot \text{m}^{-1}$), leading to easy capacity decay. Therefore, it is typically combined with highly conductive carbon materials. For example, Yang et al. [148] utilized graphene oxide (GO) and nanospherical K_xMnO_2 precursors to prepare a one-dimensional graphene nanoscroll-wrapped MnO nanoparticle (GNS@ MnO) material through a simple liquid nitrogen quenching followed by atmospheric annealing process. The obtained material exhibited a high reversible capacity of $766 \text{ mA} \cdot \text{h} \cdot \text{g}^{-1}$ at a current density of $100 \text{ mA} \cdot \text{g}^{-1}$, high rate performance ($437 \text{ mA} \cdot \text{h} \cdot \text{g}^{-1}$ at $5.0 \text{ A} \cdot \text{g}^{-1}$), and good cycling stability. Chen et al. [149] designed and synthesized one-dimensional graphene nanoscrolls wrapped with MnO nanoparticles featuring a unique nanocomposite structure. The constructed composite negative electrode material exhibits rapid ion and electron transport kinetics, as well as strong durability. When used as a negative electrode material, Co_3O_4 boasts a theoretical specific capacity of up to $890 \text{ mA} \cdot \text{h} \cdot \text{g}^{-1}$ and a low redox potential (<1 V). However, the volume expansion that occurs during charging and discharging can lead to the shedding of active materials and rapid capacity decay. To address this issue, researchers have taken various measures. For instance, Wang et al. [150] synthesized Co_3O_4 cryogels using a triblock polymer/ice crystal dual-template sol-gel method. These cryogels exhibited a specific capacitance of up to $742.3 \text{ F} \cdot \text{g}^{-1}$ and maintained 86.2% of their capacity after 2000 cycles. Liu et al. [151] successfully obtained uniformly sized and highly crystalline Co_3O_4 nanocubes with the assistance of mesoporous carbon nanorods. After heat treatment, mesoporous Co_3O_4 nanocubes were formed. Electrochemical tests revealed that the specific capacitance of the Co_3O_4 nanocube electrode was approximately $350 \text{ F} \cdot \text{g}^{-1}$ at a current density of $0.2 \text{ A} \cdot \text{g}^{-1}$.

Furthermore, the matching of electrode materials for hybrid capacitors is a crucial step in ensuring excellent capacitor performance. The compatibility of electrode materials is primarily related to their capacity, kinetics, and cycle life [152]. In the process of selecting compatible electrode materials, attention should be paid to balancing the energy density and power density of the electrode materials. It is important to choose negative and positive materials with similar physicochemical properties and consistent volume changes to enhance the stability of the cycling process. A common approach is to utilize a homologous strategy, where negative and positive materials derived from the same raw materials or undergoing similar processing procedures are selected to ensure similarity in their physicochemical properties, thereby improving material stability and compatibility. For instance, Xu et al. [153] employed a homologous strategy to prepare sulfur-doped channel carbon fiber negative electrode and active multi-channel carbon fiber positive

electrode for potassium-ion capacitors. The resulting potassium-ion capacitors achieved high energy and power densities, as well as exceptional cycling stability.

Hybrid capacitors excel in their performance due to their extensive potential window, high specific capacitance, and minimal self-discharge rate. By seamlessly integrating Faradaic and non-Faradaic processes, these capacitors are able to store a significantly larger number of charges, leading to exceptional energy and power densities. When compared to double-layer capacitors and pseudocapacitors, hybrid capacitors offer superior capacitance. Furthermore, certain hybrid capacitors are capable of operating at high voltages, albeit with slightly reduced cycling performance [110]. The overall performance of hybrid supercapacitors hinges critically on the choice of electrode and electrolyte materials. These materials have a direct bearing on the performance characteristics of the hybrid supercapacitors. Consequently, selecting suitable electrode and electrolyte materials is paramount in enhancing the overall performance of hybrid supercapacitors.

Due to the exceptional energy density exhibited by lithium ions, the integration of supercapacitors with lithium-ion storage systems holds significant importance. As a cutting-edge electrochemical energy storage solution, lithium-ion capacitors (LICs) combine the lithium-ion intercalated electrode of lithium-ion batteries with the electrical double-layer electrode of supercapacitors, offering a unique blend of benefits [154,155]. They not only inherit the high energy density advantages of batteries but also incorporate the attributes of electric double-layer capacitors, such as high power density and prolonged cycle life, thereby significantly enhancing overall performance [156–159]. The concept of LIC dates back to 1987 when Yata and his team conducted groundbreaking research on the intercalation mechanism of lithium ions in polyacene semiconductor (PAS), which was successfully commercialized as a button cell in 1989. Subsequently, in 1992, the introduction of pre-lithiation technology in PAS capacitors significantly boosted the potential of these capacitors, leaping from 2.5 V to 3.3 V. As the 21st century dawned, LIC technology witnessed significant breakthroughs. In 2001, G. G. Amatucci and his research team at Telcordia Technologies in New Jersey designed and analyzed the first modern-day lithium-ion capacitor using lithium titanate (LTO) as the negative electrode in conjunction with an activated carbon positive electrode. This device demonstrated remarkable energy performance exceeding 20 Wh/kg within a potential window of 1.5 V to 3.0 V [160]. The following year, A. D. Pasquier and his research group introduced another innovative LIC featuring an LTO negative electrode paired with a poly(fluorophenylthiophene) positive electrode, achieving a maximum deliverable power of 12 kW/kg, further expanding the application prospects of LIC [161]. In 2005, activated carbon was utilized for the first time as the negative electrode material in LIC, combined with the $\text{LiNi}_{0.5}\text{Mn}_{1.5}\text{O}_4$ positive electrode [162]. Concurrently, Fuji Heavy Industries successfully commercialized pre-lithiated PAS-based LIC. By 2008, V. Khomenko and his research team had developed a high-energy-density LIC using commercial graphite and activated carbon, significantly advancing the commercialization of LIC technology [163]. Since then, researchers in the LIC field have relentlessly explored new materials and configurations, employing graphene and doped carbon and studying their symmetric and asymmetric configurations, driving the rise of LIC as potential hybrid energy storage devices for modern applications and ultimately achieving their commercialization [164].

LIC can be applied in scenarios such as railway transportation, automatic guided vehicles, and spacecrafts, which require maintenance-free, fast charging, high power, and high energy density [165,166]. These capacitors are constructed with multiple components, including a positive electrode (typically a capacitive one), a negative electrode (commonly a pre-lithiated battery negative electrode), an electrolyte, a separator, a current collector, a conductive agent, a binder, and metallic lithium foil [167]. Each of these components contributes to the overall functionality and performance of the capacitor. Figure 20a is a digital image of a lithium-ion capacitor manufactured by JM Energy Company. Figure 20b,c show the SEM images of its negative electrode and positive electrode.

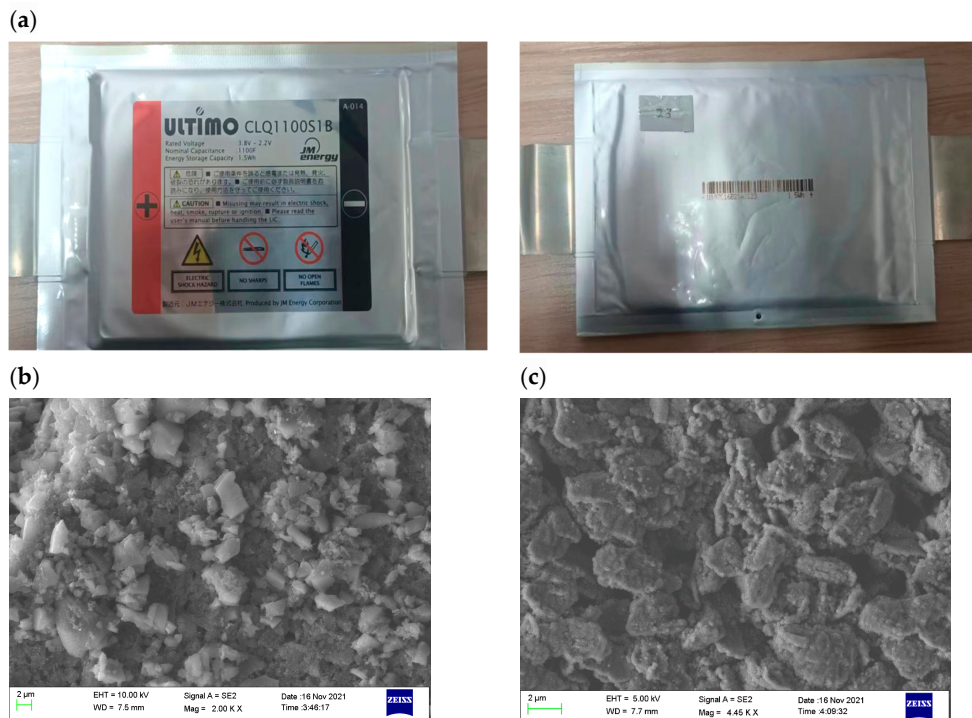


Figure 20. (a) Digital image of a soft-packaged lithium-ion capacitor manufactured by JM Energy Company. (b) An SEM image of the negative electrode. It shows that it has undergone pre-lithiation treatment. (c) An SEM image of the positive electrode, which is composed of carbon material.

The positive electrode-activated carbon material is primarily used for ion adsorption and desorption, typically prepared through carbonization and activation processes with raw materials such as coal and resin. Conversely, the negative electrode carbon material is primarily used for the insertion and extraction reactions of lithium ions, often prepared from materials like tar and asphalt through carbonization and graphitization processes. Electrolytes, the medium that facilitates ion transport between the electrodes, primarily comprise lithium salts dissolved in organic solvents. Moreover, the separator plays a crucial role as a key component, consisting of porous membranes crafted from polymers or cellulose. Its function is to avert direct contact between the positive and negative electrodes, thus safeguarding the cell's smooth and safe operation. On the other hand, the current collector, which is a thin metal foil measuring several micrometers, efficiently directs the current generated by the electrode, ensuring its effective utilization. Conductive agents, meanwhile, are tasked with establishing electronic pathways, often derived from raw materials like petroleum, through processes like cracking, carbonization, and deposition. The adhesive, a polymeric material typically synthesized artificially, plays a pivotal role in securely adhering the active material and conductive agent to the current collector. Lastly, metallic lithium foil fulfills a crucial pre-lithiation role in lithium-ion capacitor cells, with its preparation often involving the electrolysis and rolling of lithium salts. These components and materials collaborate seamlessly to guarantee the smooth operation and optimal performance of the capacitor.

The preparation flowchart of a single cell for lithium-ion capacitors is shown in Figure 21. The specific process involves mixing the positive and negative electrode materials, conductive agents, and binders and then coating them onto the current collector [168]. Subsequently, the electrodes are prepared by rolling, stripping, and slicing. These electrodes are then wound or stacked, welded, and encased. After drying, the electrolyte is injected to obtain a semi-finished cell. Finally, the semi-finished cell undergoes pre-lithiation, formation, aging, and capacity sorting to produce the final product [169]. There are various encapsulation types for lithium-ion capacitor cells. In application scenarios that require

higher energy density and power density, the electrodes are assembled into cylindrical or rectangular cells with stacking or winding methods. Common encapsulation types include cylindrical, rectangular, and pouch-type designs. When lithium-ion capacitor cells are grouped together, they can be used in fields such as power grid frequency modulation, aerospace, and rail transportation.

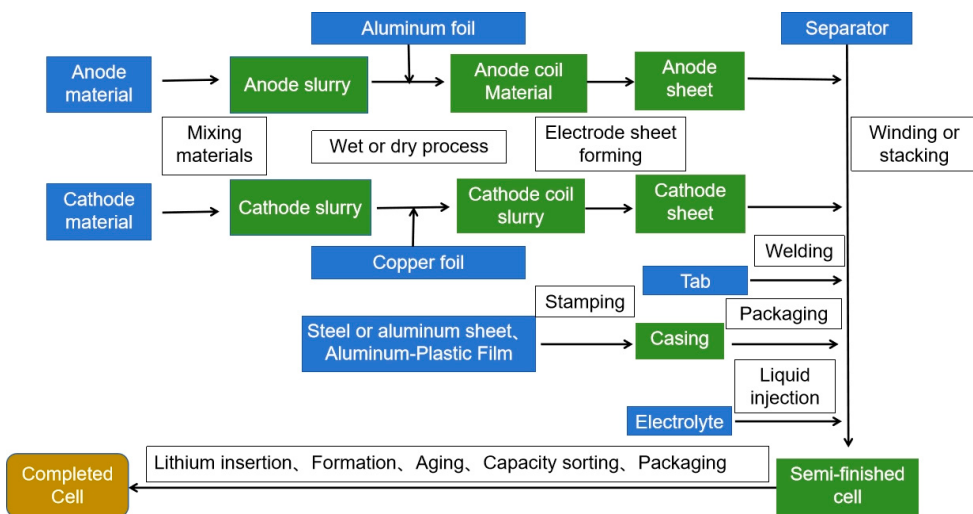


Figure 21. The preparation flowchart of a single cell for lithium-ion capacitors.

The energy storage mechanisms of the positive and negative electrodes in lithium-ion capacitors are different, and the currently common lithium-ion capacitor systems can be categorized into the following four types [170]:

- (1) The battery-type positive electrode and the capacitive-type negative electrode [171,172]. They operate through different mechanisms: electrochemical reactions occur at the positive electrode, while ion desorption processes take place at the negative electrode. During charging, lithium ions are desorbed from the positive electrode and released into the electrolyte, while simultaneously, lithium ions in the electrolyte are adsorbed onto the negative electrode, maintaining a constant ion concentration in the electrolyte. The electrolyte does not serve as an active component but merely functions as an ion carrier. However, due to the lower operating voltage, the energy density of this system is often significantly lower than other systems. Additionally, the high specific surface area of the carbon material in the negative electrode can easily lead to rapid growth of the solid electrolyte interface (SEI), resulting in poor cycling stability.
- (2) The capacitive-type positive electrode and the battery-type negative electrode [173–176]. Ion adsorption and desorption processes occur at the positive electrode, while electrochemical reactions take place at the negative electrode. During charging, anions in the electrolyte are adsorbed onto the positive electrode, while lithium ions are intercalated into the negative electrode material [177]. The ion concentration in the electrolyte decreases as the voltage increases. During discharge, the ions on the electrodes return to the electrolyte, gradually restoring the ion concentration in the electrolyte. In this system, the electrolyte serves not only as an ion carrier but also as an active component of the system. The energy density is limited by the electrode materials and the concentration of the electrolyte.
- (3) Capacitive-type positive electrode and pre-lithiated battery-type negative electrode [178,179]. The charging and discharging process of this system mainly consists of two parts: the consumption of electrolytes when the voltage is higher than the open-circuit voltage and the migration of lithium ions when the voltage is lower than the open-circuit voltage. When it is charged from the open-circuit voltage to the maximum voltage, anions in the electrolyte migrate to the positive electrode and are adsorbed onto its surface, while lithium ions are intercalated into the negative

electrode, resulting in a decrease in electrolyte ion concentration as the voltage increases. During discharge from the maximum voltage to the open-circuit voltage, anions are desorbed from the positive electrode, lithium ions are deintercalated from the negative electrode, and the electrolyte concentration returns to its initial state. When discharging from the open-circuit voltage to the minimum voltage, lithium ions stored in the negative electrode through pre-lithiation continue to be deintercalated, reducing the lithium-ion concentration in the negative electrode while gradually increasing the concentration of lithium ions adsorbed on the positive electrode. The ion concentration in the electrolyte remains basically unchanged. When charging from the minimum voltage to the open-circuit voltage, lithium ions are desorbed from the positive electrode into the electrolyte, and the lithium ions in the electrolyte are intercalated into the negative electrode. This system requires pre-intercalation of lithium into the negative electrode, which can eliminate the loss of lithium ions due to the formation of the SEI film during the initial cycle, thereby increasing the output voltage window and consequently enhancing the power density and energy density. This has become the most important category for commercialization at present.

- (4) The battery-capacitor composite positive electrode and pre-lithiated battery-type negative electrode [180,181]. The introduction of battery-type materials into the positive electrode enhances the energy density of the system, but it comes with a tradeoff in the power density and cycle life of the device. Most of the energy in this system is provided by the battery materials, making it, strictly speaking, a battery-type capacitor.

4. Summary

To clarify the differences between dielectric capacitors, electric double-layer supercapacitors, and lithium-ion capacitors, this review first introduces the classification, energy storage advantages, and application prospects of capacitors, followed by a more specific introduction to specific types of capacitors. Regarding dielectric capacitors, this review provides a detailed introduction to the classification, advantages and disadvantages, structure, energy storage principles, and manufacturing processes of thin-film capacitors, electrolytic capacitors, and ceramic capacitors. For electrochemical capacitors, an overview of their classification, structure, and energy storage principles is given, followed by a further analysis of the differences between supercapacitors and electrolytic capacitors. Subsequently, the focus is on the structural composition, production process, and energy storage principles of lithium-ion capacitors.

Currently, research on film capacitors primarily focuses on metalized organic polymer capacitors, which exhibit high charge-discharge rates, high flexibility, and excellent self-healing capabilities, promising good application prospects in areas such as microwave communications, hybrid electric vehicles, and renewable energy. However, they face challenges in terms of relatively poor thermal stability and high production costs. In the future, more research should be conducted on multiphase/multicomponent high-temperature dielectric polymers, including blend polymers and multilayer polymers, to enhance their high-temperature performance. Additionally, advanced film technologies should be developed, and processing techniques optimized to reduce costs [182]. Electrolytic capacitors are known for their large capacitance and high volumetric efficiency, making them suitable for applications in electronic devices or as energy buffers. However, they suffer from drawbacks such as high equivalent series resistance (ESR) and relatively short service life. Therefore, future efforts should be directed toward the development of novel polymer-based electrolytic capacitors, accompanied by in-depth studies on their failure mechanisms and prediction methods to extend their service life. Research on ceramic capacitors primarily focuses on MLCC. These capacitors exhibit extremely low ESR and equivalent series inductance, coupled with high current-handling capabilities and outstanding high-temperature stability. As a result, they show immense potential for applications in electric vehicles, 5G base stations, clean energy generation, smart grids, and other fields. Future

research in ceramic capacitors can focus on utilizing dielectric materials like antiferroelectric materials or barium titanate-based compounds. By optimizing their electrode structures or manufacturing processes, researchers aim to enhance the breakdown strength, dielectric stability, and energy density of ceramic capacitors, further expanding their capabilities and applications [183]. For supercapacitors, their high-power density and low energy density have made enhancing energy density a persistent research focus. Additionally, with the rapid development of flexible electronics technology, there has been a surge in the development of smart clothing and portable electronic devices, and flexible supercapacitors have demonstrated vast application prospects in areas such as flexible displays, wearable electronic devices, and portable biomedical monitoring devices. Therefore, in the future, significant efforts can be directed toward utilizing novel materials like metal-organic frameworks (MOFs), covalent organic frameworks (COFs), and hydrogen-bonded organic frameworks (HOFs) in supercapacitors to improve their chemical stability and energy density. Furthermore, the development of flexible supercapacitor electrode materials with good stability, excellent performance, and long service life is also a crucial direction for the future advancement of supercapacitors. For lithium-ion capacitors, future research should emphasize the exploration of new electrode materials like two-dimensional MXenes to enhance their energy density. Additionally, optimizing the pre-lithiation process of lithium-ion capacitors and improving the compatibility of pre-lithiation technology are also essential steps toward their further development.

Author Contributions: W.L.: Conceptualization, methodology, investigation, writing—original draft. X.S.: conceptualization, supervision, investigation, and writing—review and editing. X.Y.: investigation, methodology and resources. Y.G.: supervision, investigation, and writing—review and editing. X.Z.: supervision, investigation, and writing—review and editing. K.W.: methodology and resources. Y.M.: supervision, investigation, methodology, and writing—review and editing. All authors have read and agreed to the published version of the manuscript.

Funding: This research received no external funding.

Data Availability Statement: The original contributions presented in the study are included in the article; further inquiries can be directed to the corresponding author/s.

Acknowledgments: We are grateful to the Institute of Electrical Engineering, Chinese Academy of Sciences, for providing us with capacitors and experimental equipment.

Conflicts of Interest: The author Xinyu Yan was employed by the TBEA Sunoasis Co., Ltd. All authors declare that the research was conducted in the absence of any commercial or financial relationships that could be construed as a potential conflict of interest.

References

1. Adediji, Y.B.; Adeyinka, A.M.; Yahya, D.I.; Mbelu, O.V. A review of energy storage applications of lead-free BaTiO₃-based dielectric ceramic capacitors. *Energy Ecol. Environ.* **2023**, *8*, 401–419. [[CrossRef](#)]
2. Li, C.; Zhang, X.; Wang, K.; Su, F.Y.; Chen, C.M.; Liu, F.Y.; Wu, Z.S.; Ma, Y.W. Recent advances in carbon nanostructures prepared from carbon dioxide for high-performance supercapacitors. *J. Energy Chem.* **2021**, *54*, 352–367. [[CrossRef](#)]
3. Agajie, T.F.; Ali, A.; Fopah-Lele, A.; Amoussou, I.; Khan, B.; Velasco, C.L.R.; Tanyi, E. A Comprehensive Review on Techno-Economic Analysis and Optimal Sizing of Hybrid Renewable Energy Sources with Energy Storage Systems. *Energies* **2023**, *16*, 642. [[CrossRef](#)]
4. Deka, B.; Cho, K.-H. BiFeO₃-Based Relaxor Ferroelectrics for Energy Storage: Progress and Prospects. *Materials* **2021**, *14*, 7188. [[CrossRef](#)]
5. Sayed, E.T.; Olabi, A.G.; Alami, A.H.; Radwan, A.; Mdallal, A.; Rezk, A.; Abdelkareem, M.A. Renewable Energy and Energy Storage Systems. *Energies* **2023**, *16*, 1415. [[CrossRef](#)]
6. Xu, Y.; Wang, K.; Zhang, X.; Ma, Y.; Peng, Q.; Gong, Y.; Yi, S.; Guo, H.; Zhang, X.; Sun, X. Improved Li-Ion Conduction and (Electro) Chemical Stability at Garnet-Polymer Interface through Metal-Nitrogen Bonding. *Adv. Energy Mater.* **2023**, *13*, 2204377. [[CrossRef](#)]
7. Yang, L.; Kong, X.; Li, F.; Hao, H.; Cheng, Z.; Liu, H.; Li, J.-F.; Zhang, S. Perovskite lead-free dielectrics for energy storage applications. *Prog. Mater. Sci.* **2019**, *102*, 72–108. [[CrossRef](#)]
8. Navarro, G.; Torres, J.; Blanco, M.; Nájera, J.; Santos-Herran, M.; Lafoz, M. Present and Future of Supercapacitor Technology Applied to Powertrains, Renewable Generation and Grid Connection Applications. *Energies* **2021**, *14*, 3060. [[CrossRef](#)]

9. Liu, L.M.; Qu, J.L.; Gu, A.J.; Wang, B.H. Percolative polymer composites for dielectric capacitors: A brief history, materials, and multilayer interface design. *J. Mater. Chem. A* **2020**, *8*, 18515–18537. [[CrossRef](#)]
10. Conte, M. Supercapacitors Technical Requirements for New Applications. *Fuel Cells* **2010**, *10*, 806–818. [[CrossRef](#)]
11. Aravindan, V.; Gnanaraj, J.; Lee, Y.-S.; Madhavi, S. Insertion-Type Electrodes for Nonaqueous Li-Ion Capacitors. *Chem. Rev.* **2014**, *114*, 11619–11635. [[CrossRef](#)]
12. Fitzgerald, D. Improvements in electrical condensers or accumulators. *Br. Pat.* **1876**, *3466*, 1876.
13. McLean, D. Metallized paper for capacitors. *Proc. IRE* **1950**, *38*, 1010–1014. [[CrossRef](#)]
14. McLean, D.; Wehe, H. Miniature lacquer film capacitors. *Proc. IRE* **1954**, *42*, 1799–1805. [[CrossRef](#)]
15. Ho, J.; Jow, T.R.; Boggs, S. Historical introduction to capacitor technology. *IEEE Electr. Insul. Mag.* **2010**, *26*, 20–25. [[CrossRef](#)]
16. Simon, P.; Gogotsi, Y. Materials for electrochemical capacitors. *Nat. Mater.* **2008**, *7*, 845–854. [[CrossRef](#)]
17. Dong, J.-F.; Deng, X.-L.; Niu, Y.-J.; Pan, Z.-Z.; Wang, H. Research progress of polymer based dielectrics for high-temperature capacitor energy storage. *Acta Physica Sinica* **2020**, *69*, 217701. [[CrossRef](#)]
18. MacDougall, F.W.; Ennis, J.B.; Cooper, R.A.; Bates, J.; Seal, K. High energy density pulsed power capacitors. In Proceedings of the 14th IEEE International Pulsed Power Conference, Dallas, TX, USA, 15–18 June 2003; pp. 513–517.
19. Prateek; Thakur, V.K.; Gupta, R.K. Recent Progress on Ferroelectric Polymer-Based Nanocomposites for High Energy Density Capacitors: Synthesis, Dielectric Properties, and Future Aspects. *Chem. Rev.* **2016**, *116*, 4260–4317. [[CrossRef](#)]
20. Singh, M.; Apata, I.E.; Samant, S.; Wu, W.J.; Tawade, B.V.; Pradhan, N.; Raghavan, D.; Karim, A. Nanoscale Strategies to Enhance the Energy Storage Capacity of Polymeric Dielectric Capacitors: Review of Recent Advances. *Polym. Rev.* **2022**, *62*, 211–260. [[CrossRef](#)]
21. Dang, Z.-M. Polymer nanocomposites with high permittivity. In *Nanocrystalline Materials*; Elsevier: Amsterdam, The Netherlands, 2014; pp. 305–333.
22. Sherrill, S.A.; Banerjee, P.; Rubloff, G.W.; Lee, S.B. High to ultra-high power electrical energy storage. *Phys. Chem. Chem. Phys.* **2011**, *13*, 20714–20723. [[CrossRef](#)]
23. Sun, L.; Shi, Z.C.; Liang, L.; Wei, S.; Wang, H.L.; Dastan, D.; Sun, K.; Fan, R.H. Layer-structured BaTiO₃/P(VDF-HFP) composites with concurrently improved dielectric permittivity and breakdown strength toward capacitive energy-storage applications. *J. Mater. Chem. C* **2020**, *8*, 10257–10265. [[CrossRef](#)]
24. Fan, X.; Wang, J.; Yuan, H.; Zheng, Z.; Zhang, J.; Zhu, K. Multi-scale synergic optimization strategy for dielectric energy storage ceramics. *J. Adv. Ceram.* **2023**, *12*, 649–680. [[CrossRef](#)]
25. Yang, M.; Guo, M.; Xu, E.; Ren, W.; Wang, D.; Li, S.; Zhang, S.; Nan, C.-W.; Shen, Y. Polymer nanocomposite dielectrics for capacitive energy storage. *Nat. Nanotechnol.* **2024**, *19*, 588–603. [[CrossRef](#)]
26. Xiao, M.; Zhang, Z.; Du, B. Dielectric performance improvement of polypropylene film by hierarchical structure design for metallized film capacitors. *J. Phys. D Appl. Phys.* **2024**, *57*, 385501. [[CrossRef](#)]
27. Hu, T.-Y.; Ma, C.; Cheng, S.-d.; Hu, G.; Liu, M. Ultrahigh-temperature capacitors realized by controlling polarization behavior in relaxor ferroelectric. *Chem. Eng. J.* **2024**, *492*, 152365. [[CrossRef](#)]
28. Gnonhoue, O.G.; Velazquez-Salazar, A.; David, É.; Preda, I. Review of Technologies and Materials Used in High-Voltage Film Capacitors. *Polymers* **2021**, *13*, 766. [[CrossRef](#)]
29. Reuter, R.C., Jr.; Allen, J.J. Prediction of Mechanical States in Wound Capacitors. *J. Mech. Des.* **1991**, *113*, 387–392. [[CrossRef](#)]
30. Sarjeant, W.J.; Zirnheld, J.; MacDougall, F.W. Capacitors. *IEEE Trans. Plasma Sci.* **1998**, *26*, 1368–1392. [[CrossRef](#)]
31. Tahalyani, J.; Akhtar, M.J.; Cherusseri, J.; Kar, K.K. Characteristics of Capacitor: Fundamental Aspects. In *Handbook of Nanocomposite Supercapacitor Materials I: Characteristics*; Kar, K.K., Ed.; Springer International Publishing: Cham, Switzerland, 2020; pp. 1–51.
32. Fan, B.H.; Zhou, M.Y.; Zhang, C.; He, D.L.; Bai, J.B. Polymer-based materials for achieving high energy density film capacitors. *Prog. Polym. Sci.* **2019**, *97*, 101143. [[CrossRef](#)]
33. Xiong, J.; Wang, X.; Zhang, X.; Xie, Y.C.; Lu, J.Y.; Zhang, Z.C. How the biaxially stretching mode influence dielectric and energy storage properties of polypropylene films. *J. Appl. Polym. Sci.* **2021**, *138*, 50029. [[CrossRef](#)]
34. Streibl, M.; Karmazin, R.; Moos, R. Materials and applications of polymer films for power capacitors with special respect to nanocomposites. *IEEE Trans. Dielectr. Electr. Insul.* **2018**, *25*, 2429–2442. [[CrossRef](#)]
35. Ran, Z.Y.; Du, B.X.; Xiao, M.; Li, J. Crystallization Morphology-Dependent Breakdown Strength of Polypropylene Films for Converter Valve Capacitor. *IEEE Trans. Dielectr. Electr. Insul.* **2021**, *28*, 964–971. [[CrossRef](#)]
36. Ping, J.-B.; Feng, Q.-K.; Zhang, Y.-X.; Wang, X.-J.; Huang, L.; Zhong, S.-L.; Dang, Z.-M. A Bilayer High-Temperature Dielectric Film with Superior Breakdown Strength and Energy Storage Density. *Nano-Micro Lett.* **2023**, *15*, 154. [[CrossRef](#)]
37. Zou, C.; Zhang, Q.; Zhang, S.; Kushner, D.; Zhou, X.; Bernard, R.; Orchard, R.J., Jr. PEN/Si₃N₄ bilayer film for dc bus capacitors in power converters in hybrid electric vehicles. *J. Vac. Sci. Technol. B* **2011**, *29*, 061401. [[CrossRef](#)]
38. Zhang, C.; Yan, W.; Zhang, T.; Zhang, T.; Zhang, Y.; Tang, C.; Chi, Q. Sandwich-Structured PC/PVDF-Based Energy Storage Dielectric with Inorganic Doping to Regulate Electric Field Distribution. *J. Phys. Chem. C* **2024**, *128*, 5717–5730. [[CrossRef](#)]
39. Reed, C.W.; Cichanowski, S.W. The Fundamentals of Aging in HV Polymer-Film Capacitors. *IEEE Trans. Dielectr. Electr. Insul.* **1994**, *1*, 904–922. [[CrossRef](#)]

40. Feng, M.N.; Chen, M.; Qiu, J.; He, M.; Huang, Y.M.; Lin, J. Improving dielectric properties of poly(arylene ether nitrile) composites by employing core-shell structured BaTiO₃@polydopamine and MoS₂@polydopamine interlinked with poly(ethylene imine) for high-temperature applications. *J. Alloys Compd.* **2021**, *856*, 158213. [CrossRef]
41. Valentine, N.; Azarian, M.H.; Pecht, M. Metallized film capacitors used for EMI filtering: A reliability review. *Microelectron. Reliab.* **2019**, *92*, 123–135. [CrossRef]
42. Ho, J.S.; Greenbaum, S.G. Polymer Capacitor Dielectrics for High Temperature Applications. *ACS Appl. Mater. Interfaces* **2018**, *10*, 29189–29218. [CrossRef]
43. Li, Q.; Cheng, S. Polymer nanocomposites for high-energy-density capacitor dielectrics: Fundamentals and recent progress. *IEEE Electr. Insul. Mag.* **2020**, *36*, 7–28. [CrossRef]
44. Rabuffi, M.; Picci, G. Status quo and future prospects for metallized polypropylene energy storage capacitors. *IEEE Trans. Plasma Sci.* **2002**, *30*, 1939–1942. [CrossRef]
45. Bai, G.; Chen, Z.; Liu, J.; Wang, F.; Zhang, Y. Microstructure Evolution and Performance Enhancement of Sintered Aluminum Foils for Aluminum Electrolytic Capacitors. *J. Electron. Mater.* **2024**, *53*, 2026–2039. [CrossRef]
46. Zeng, X.; Bian, J.; Liang, L.; Cao, Q.; Liu, L.; Chen, X.; Wang, Y.; Xie, X.; Xie, G. Preparation and characterization of anode foil for aluminum electrolytic capacitors by powder additive manufacturing. *Powder Technol.* **2023**, *426*, 118602. [CrossRef]
47. Chen, D.; Fu, J.; Huang, S.; Huang, J.; Yang, J.; Ren, S.; Ma, J. Design of La-based MG-Ta composite with high and tailorable properties for solid Ta electrolytic capacitor. *Mater. Des.* **2024**, *238*, 112743. [CrossRef]
48. Narale, S.B.; Verma, A.; Anand, S. Structure and Degradation of Aluminum Electrolytic Capacitors. In Proceedings of the 2019 National Power Electronics Conference (NPEC), Tiruchirappalli, India, 13–15 December 2019; pp. 1–6.
49. Bramouille, M. Electrolytic or film capacitors? In Proceedings of the Conference Record of 1998 IEEE Industry Applications Conference. Thirty-Third IAS Annual Meeting (Cat. No.98CH36242), St. Loius, MI, USA, 12–15 October 1998; Volume 1132, pp. 1138–1141.
50. Torki, J.; Joubert, C.; Sari, A. Electrolytic capacitor: Properties and operation. *J. Energy Storage* **2023**, *58*, 106330. [CrossRef]
51. EPCOS, A. Aluminum Electrolytic Capacitors—General Technical Information. 2019. Available online: <https://www.tdk-electronics.tdk.com/download/185386/e724fb43668a157bc547c65b0cff75f8/pdf-generaltechnicalinformation.pdf> (accessed on 3 May 2024).
52. Chen, X.; Xi, L.; Zhang, Y.; Ma, H.; Huang, Y.; Chen, Y. Fractional techniques to characterize non-solid aluminum electrolytic capacitors for power electronic applications. *Nonlinear Dyn.* **2019**, *98*, 3125–3141. [CrossRef]
53. Both, J. The modern era of aluminum electrolytic capacitors. *IEEE Electr. Insul. Mag.* **2015**, *31*, 24–34. [CrossRef]
54. Film, F.C.M.P. 1. General Description of Aluminum Electrolytic Capacitors. 2015. Available online: <https://www.nichicon.co.jp/english/products/pdf/aluminum.pdf> (accessed on 3 May 2024).
55. McLean, D.A.; Power, F.S. Tantalum Solid Electrolytic Capacitors. *Proc. IRE* **1956**, *44*, 872–878. [CrossRef]
56. Freeman, Y.; Lessner, P.; Luzinov, I. Reliability and Failure Mode in Solid Tantalum Capacitors. *Ecs J. Solid State Sci. Technol.* **2021**, *10*, 045007. [CrossRef]
57. Nishino, A. Capacitors: Operating principles, current market and technical trends. *J. Power Sources* **1996**, *60*, 137–147. [CrossRef]
58. Romero, J.A.; Azarian, M.H.; Pecht, M. Life model for tantalum electrolytic capacitors with conductive polymers. *Microelectron. Reliab.* **2020**, *104*, 113550. [CrossRef]
59. Gill, J. Basic Tantalum Capacitor Technology. Available online: <https://kyocera-avx.com/docs/techinfo/Tantalum-NiobiumCapacitors/bsctant.pdf> (accessed on 3 May 2024).
60. Freeman, Y. Basic Technology. In *Tantalum and Niobium-Based Capacitors: Science, Technology, and Applications*; Freeman, Y., Ed.; Springer International Publishing: Cham, Switzerland, 2022; pp. 23–52.
61. Kaiser, C.J. *The Capacitor Handbook*; Springer Science & Business Media: Berlin/Heidelberg, Germany, 2012.
62. Teverovsky, A. Breakdown and Self-healing in Tantalum Capacitors. *IEEE Trans. Dielectr. Electr. Insul.* **2021**, *28*, 663–671. [CrossRef]
63. Jia, W.X.; Hou, Y.D.; Zheng, M.P.; Xu, Y.R.; Zhu, M.K.; Yang, K.Y.; Cheng, H.R.; Sun, S.Y.; Xing, J. Advances in lead-free high-temperature dielectric materials for ceramic capacitor applicationInspec keywordsOther keywords. *Iet Nanodielectr.* **2018**, *1*, 3–16. [CrossRef]
64. Randall, M.-J.P.C.A. A brief introduction to ceramic capacitors. *IEEE Electr. Insul. Mag.* **2010**, *26*, 44–50. [CrossRef]
65. Park, Y.; Park, J.J.; Park, K.S.; Hong, Y.M.; Lee, E.J.; Kim, S.O.; Lee, J.H. Enhancement of Mechanical Properties of Multilayer Ceramic Capacitors through a BaTiO₃/polydopamine Cover Layer. *Polymers* **2023**, *15*, 4014. [CrossRef]
66. Lv, Z.; Lu, T.; Liu, Z.; Hu, T.; Hong, Z.; Guo, S.; Xu, Z.; Song, Y.; Chen, Y.; Zhao, X.; et al. NaNbO₃-Based Multilayer Ceramic Capacitors with Ultrahigh Energy Storage Performance. *Adv. Energy Mater.* **2024**, *14*, 2304291. [CrossRef]
67. Van Trinh, H.; Talbot, J.B. Electrodeposition Method for Terminals of Multilayer Ceramic Capacitors. *J. Am. Ceram. Soc.* **2004**, *86*, 905–909. [CrossRef]
68. Wojewoda, L.E.; Hill, M.J.; Radhakrishnan, K.; Goyal, N. Use Condition Characterization of MLCCs. *IEEE Trans. Adv. Packag.* **2009**, *32*, 109–115. [CrossRef]
69. Gong, H.; Wang, X.; Tian, Z.; Zhang, H.; Li, L. Interfacial diffusion behavior in Ni-BaTiO₃ MLCCs with ultra-thin active layers. *Electron. Mater. Lett.* **2014**, *10*, 417–421. [CrossRef]

70. Sumithra, S.; Annapoorni, K.; Ellmore, A.; Vaidhyanathan, B. Microwave assisted processing of X8R nanocrystalline BaTiO₃ based ceramic capacitors and multilayer devices. *Open Ceram.* **2022**, *9*, 100214. [[CrossRef](#)]
71. Wang, Y.Q.; Ko, B.H.; Jeong, S.G.; Park, K.S.; Park, N.C.; Park, Y.P. Analysis of the influence of soldering parameters on multi-layer ceramic capacitor vibration. *Microsyst. Technol.-Micro-Nanosyst.-Inf. Storage Process. Syst.* **2015**, *21*, 2565–2571. [[CrossRef](#)]
72. Hong, K.; Lee, T.H.; Suh, J.M.; Yoon, S.H.; Jang, H.W. Perspectives and challenges in multilayer ceramic capacitors for next generation electronics. *J. Mater. Chem. C* **2019**, *7*, 9782–9802. [[CrossRef](#)]
73. Zhang, H.B.; Wei, T.; Zhang, Q.; Ma, W.G.; Fan, P.Y.; Salamon, D.; Zhang, S.T.; Nan, B.; Tan, H.; Ye, Z.G. A review on the development of lead-free ferroelectric energy-storage ceramics and multilayer capacitors. *J. Mater. Chem. C* **2020**, *8*, 16648–16667. [[CrossRef](#)]
74. Gurav, A.; Xu, X.; Freeman, Y.; Reed, E. KEMET Electronics: Breakthroughs in Capacitor Technology. In *Materials Research for Manufacturing: An Industrial Perspective of Turning Materials into New Products*; Madsen, L.D., Svedberg, E.B., Eds.; Springer International Publishing: Cham, Switzerland, 2016; pp. 93–129.
75. Laadjal, K.; Cardoso, A.J.M. Multilayer Ceramic Capacitors: An Overview of Failure Mechanisms, Perspectives, and Challenges. *Electronics* **2023**, *12*, 1297. [[CrossRef](#)]
76. Miller, J.R. Perspective on electrochemical capacitor energy storage. *Appl. Surf. Sci.* **2018**, *460*, 3–7. [[CrossRef](#)]
77. Zheng, L.X.; Xu, P.H.; Zhao, Y.J.; Peng, J.X.; Yang, P.J.; Shi, X.W.; Zheng, H.J. Unique core-shell Co₂(OH)₂CO₃@MOF nanoarrays with remarkably improved cycling life for high performance pseudocapacitors. *Electrochim. Acta* **2022**, *412*, 140142. [[CrossRef](#)]
78. Yi, S.; Wang, L.; Zhang, X.; Li, C.; Xu, Y.A.; Wang, K.; Sun, X.Z.; Ma, Y.W. Recent advances in MXene-based nanocomposites for supercapacitors. *Nanotechnology* **2023**, *34*, 432001. [[CrossRef](#)]
79. Zhao, J.; Burke, A.F. Review on supercapacitors: Technologies and performance evaluation. *J. Energy Chem.* **2021**, *59*, 276–291. [[CrossRef](#)]
80. Liu, Y.; Shearing, P.R.; He, G.; Brett, D.J.L. Supercapacitors: History, Theory, Emerging Technologies, and Applications. In *Advances in Sustainable Energy: Policy, Materials and Devices*; Gao, Y.-j., Song, W., Liu, J.L., Bashir, S., Eds.; Springer International Publishing: Cham, Switzerland, 2021; pp. 417–449.
81. Chen, Z.; Yu, D.; Xiong, W.; Liu, P.; Liu, Y.; Dai, L. Graphene-Based Nanowire Supercapacitors. *Langmuir* **2014**, *30*, 3567–3571. [[CrossRef](#)]
82. Snook, G.A.; Kao, P.; Best, A.S. Conducting-polymer-based supercapacitor devices and electrodes. *J. Power Sources* **2011**, *196*, 1–12. [[CrossRef](#)]
83. Becker, H. Low Voltage Electrolytic Capacitor. U. S. Patent 2,800,616A, 23 July 1957.
84. Shirakawa, H.; Louis, E.J.; MacDiarmid, A.G.; Chiang, C.K.; Heeger, A.J. Synthesis of electrically conducting organic polymers: Halogen derivatives of polyacetylene, (CH) x. *J. Chem. Soc. Chem. Commun.* **1977**, 578–580. [[CrossRef](#)]
85. Sun, J.; Luo, B.; Li, H. A Review on the Conventional Capacitors, Supercapacitors, and Emerging Hybrid Ion Capacitors: Past, Present, and Future. *Adv. Energy Sustain. Res.* **2022**, *3*, 2100191. [[CrossRef](#)]
86. Zan, G.; Li, S.; Chen, P.; Dong, K.; Wu, Q.; Wu, T. Mesoporous Cubic Nanocages Assembled by Coupled Monolayers With 100% Theoretical Capacity and Robust Cycling. *ACS Cent. Sci.* **2024**, *10*, 1283–1294. [[CrossRef](#)]
87. Shwetha, K.P.; Manjunatha, C.; Sudha Kamath, M.K.; Vinaykumar; Radhika, M.G.R.; Khosla, A. Morphology-controlled synthesis and structural features of ultrafine nanoparticles of Co₃O₄: An active electrode material for a supercapacitor. *Appl. Res.* **2022**, *1*, e20220031. [[CrossRef](#)]
88. Luo, Q.; Lu, C.; Liu, L.; Zhu, M. Triethanolamine assisted synthesis of bimetallic nickel cobalt nitride/nitrogen-doped carbon hollow nanoflowers for supercapacitor. *Microstructures* **2023**, *3*, 2023011.
89. Wang, T.; Wang, Y.; Lei, J.; Chen, K.-J.; Wang, H. Electrochemically induced surface reconstruction of Ni-Co oxide nanosheet arrays for hybrid supercapacitors. *Exploration* **2021**, *1*, 20210178. [[CrossRef](#)]
90. Song, H.; Wang, Y.; Fei, Q.; Nguyen, D.H.; Zhang, C.; Liu, T. Cryopolymerization-enabled self-wrinkled polyaniline-based hydrogels for highly stretchable all-in-one supercapacitors. *Exploration* **2022**, *2*, 20220006. [[CrossRef](#)]
91. Huai, X.; Liu, J.; Wu, X. Cobalt-doped NiMoO₄ nanosheet for high-performance flexible supercapacitor. *Chin. J. Struct. Chem.* **2023**, *42*, 100158. [[CrossRef](#)]
92. Liu, B.; Cao, Z.; Yang, Z.; Qi, W.; He, J.; Pan, P.; Li, H.; Zhang, P. Flexible micro-supercapacitors fabricated from MnO₂ nanosheet/graphene composites with black phosphorus additive. *Prog. Nat. Sci. Mater. Int.* **2022**, *32*, 10–19. [[CrossRef](#)]
93. Zhu, R.-J.; Liu, J.; Hua, C.; Pan, H.-Y.; Cao, Y.-J.; Li, M. Preparation of vanadium-based electrode materials and their research progress in solid-state flexible supercapacitors. *Rare Met.* **2024**, *43*, 431–454. [[CrossRef](#)]
94. Wang, T.; Hu, S.; Hu, Y.; Wu, D.; Wu, H.; Huang, J.; Wang, H.; Zhao, W.; Yu, W.; Wang, M.; et al. Biologically inspired anthraquinone redox centers and biomass graphene for renewable colloidal gels toward ultrahigh-performance flexible micro-supercapacitors. *J. Mater. Sci. Technol.* **2023**, *151*, 178–189. [[CrossRef](#)]
95. Li, J.; Dong, Z.; Chen, R.; Wu, Q.; Zan, G. Advanced nickel-based composite materials for supercapacitor electrodes. *Ionics* **2024**, *30*, 1833–1855. [[CrossRef](#)]
96. Troschke, E.; Oschatz, M.; Ilic, I.K. Schiff-bases for sustainable battery and supercapacitor electrodes. *Exploration* **2021**, *1*, 20210128. [[CrossRef](#)] [[PubMed](#)]
97. Shi, J.; Tian, X.; Yang, T.; Hu, S.; Liu, Z. Redox electrolyte-enhanced carbon-based supercapacitors: Recent advances and future perspectives. *Energy Mater. Devices* **2023**, *1*, 9370009. [[CrossRef](#)]

98. Wu, X.; Liu, R.; Zhao, J.; Fan, Z. Advanced carbon materials with different spatial dimensions for supercapacitors. *Nano Mater. Sci.* **2021**, *3*, 241–267. [[CrossRef](#)]
99. Kong, D.; Lv, W.; Liu, R.; He, Y.-B.; Wu, D.; Li, F.; Fu, R.; Yang, Q.-H.; Kang, F. Superstructured carbon materials: Design and energy applications. *Energy Mater. Devices* **2023**, *1*, 9370017. [[CrossRef](#)]
100. Wang, G.; Zhang, L.; Zhang, J. A review of electrode materials for electrochemical supercapacitors. *Chem. Soc. Rev.* **2012**, *41*, 797–828. [[CrossRef](#)] [[PubMed](#)]
101. Zhou, W.; Liu, Z.; Chen, W.; Sun, X.; Luo, M.; Zhang, X.; Li, C.; An, Y.; Song, S.; Wang, K. A Review on Thermal Behaviors and Thermal Management Systems for Supercapacitors. *Batteries* **2023**, *9*, 128. [[CrossRef](#)]
102. Shukla, A.K.; Banerjee, A.; Ravikumar, M.K.; Jalajakshi, A. Electrochemical capacitors: Technical challenges and prognosis for future markets. *Electrochim. Acta* **2012**, *84*, 165–173. [[CrossRef](#)]
103. Terasawa, N.; Asaka, K. High-Performance Hybrid (Electrostatic Double-Layer and Faradaic Capacitor-Based) Polymer Actuators Incorporating Nickel Oxide and Vapor-Grown Carbon Nanofibers. *Langmuir* **2014**, *30*, 14343–14351. [[CrossRef](#)]
104. Mohd Abdah, M.A.A.; Azman, N.H.N.; Kulandaivalu, S.; Sulaiman, Y. Review of the use of transition-metal-oxide and conducting polymer-based fibres for high-performance supercapacitors. *Mater. Des.* **2020**, *186*, 108199. [[CrossRef](#)]
105. Choi, H.; Yoon, H. Nanostructured electrode materials for electrochemical capacitor applications. *Nanomaterials* **2015**, *5*, 906–936. [[CrossRef](#)] [[PubMed](#)]
106. Pal, B.; Yang, S.; Ramesh, S.; Thangadurai, V.; Jose, R. Electrolyte selection for supercapacitive devices: A critical review. *Nanoscale Adv.* **2019**, *1*, 3807–3835. [[CrossRef](#)] [[PubMed](#)]
107. Zhang, L.L.; Zhao, X.S. Carbon-based materials as supercapacitor electrodes. *Chem. Soc. Rev.* **2009**, *38*, 2520–2531. [[CrossRef](#)] [[PubMed](#)]
108. Brza, M.A.; Aziz, S.B.; Anuar, H.; Ali, F.; Hamsan, M.H.; Kadir, M.F.Z.; Abdulwahid, R.T. Metal framework as a novel approach for the fabrication of electric double layer capacitor device with high energy density using plasticized Poly(vinyl alcohol): Ammonium thiocyanate based polymer electrolyte. *Arab. J. Chem.* **2020**, *13*, 7247–7263. [[CrossRef](#)]
109. Yao, F.; Pham, D.T.; Lee, Y.H. Carbon-Based Materials for Lithium-Ion Batteries, Electrochemical Capacitors, and Their Hybrid Devices. *ChemSusChem* **2015**, *8*, 2284–2311. [[CrossRef](#)]
110. Banerjee, S.; Sinha, P.; Verma, K.D.; Pal, T.; De, B.; Cherusseri, J.; Manna, P.K.; Kar, K.K. Capacitor to Supercapacitor. In *Handbook of Nanocomposite Supercapacitor Materials I: Characteristics*; Kar, K.K., Ed.; Springer International Publishing: Cham, Switzerland, 2020; pp. 53–89.
111. Forse, A.C.; Merlet, C.; Griffin, J.M.; Grey, C.P. New Perspectives on the Charging Mechanisms of Supercapacitors. *J. Am. Chem. Soc.* **2016**, *138*, 5731–5744. [[CrossRef](#)]
112. Frackowiak, E.; Béguin, F. Carbon materials for the electrochemical storage of energy in capacitors. *Carbon* **2001**, *39*, 937–950. [[CrossRef](#)]
113. Bizuneh, G.G.; Adam, A.M.M.; Ma, J. Progress on carbon for electrochemical capacitors. *Battery Energy* **2023**, *2*, 20220021. [[CrossRef](#)]
114. Li, C.; Zhang, X.; Lv, Z.S.; Wang, K.; Sun, X.Z.; Chen, X.D.; Ma, Y.W. Scalable combustion synthesis of graphene-welded activated carbon for high-performance supercapacitors. *Chem. Eng. J.* **2021**, *414*, 128781. [[CrossRef](#)]
115. Du, C.; Yeh, J.; Pan, N. High power density supercapacitors using locally aligned carbon nanotube electrodes. *Nanotechnology* **2005**, *16*, 350. [[CrossRef](#)]
116. Stoller, M.D.; Park, S.; Zhu, Y.; An, J.; Ruoff, R.S. Graphene-Based Ultracapacitors. *Nano Lett.* **2008**, *8*, 3498–3502. [[CrossRef](#)]
117. Yu, X.; Lu, B.; Xu, Z. Super Long-Life Supercapacitors Based on the Construction of Nanohoneycomb-Like Strongly Coupled CoMoO₄-3D Graphene Hybrid Electrodes. *Adv. Mater.* **2014**, *26*, 990. [[CrossRef](#)]
118. Fu, G.; Li, H.; Bai, Q.; Li, C.; Shen, Y.; Uyama, H. Dual-doping activated carbon with hierarchical pore structure derived from polymeric porous monolith for high performance EDLC. *Electrochim. Acta* **2021**, *375*, 137927. [[CrossRef](#)]
119. Lv, X.W.; Ji, S.; Wang, Z.H.; Wang, X.Y.; Wang, H.; Wang, R.F. Fabrication of highly-conductive porous capacitor electrodes by the insertion of Cu-nanoparticles into N-doped flocculated carbon catalysts. *J. Colloid Interface Sci.* **2022**, *610*, 106–115. [[CrossRef](#)]
120. Yoo, J.; Yang, I.; Kwon, D.; Jung, M.; Kim, M.-S.; Jung, J.C. Low-Cost Carbon Xerogels Derived from Phenol–Formaldehyde Resin for Organic Electric Double-Layer Capacitors. *Energy Technol.* **2021**, *9*, 2000918. [[CrossRef](#)]
121. Thirumurugan, A.; Ramakrishnan, K.; Ramadoss, A.; Thandapani, P.; Thangavelu, P.; Udayabhaskar, R.; Morel, M.J.; Dhanabalan, S.S.; Dineshbabu, N.; Ravichandran, K.; et al. Nanostructured Materials for Supercapacitors. In *Nanostructured Materials for Supercapacitors*; Thomas, S., Gueye, A.B., Gupta, R.K., Eds.; Springer International Publishing: Cham, Switzerland, 2022; pp. 1–26.
122. Ates, M.; Chebil, A.; Yoruk, O.; Dridi, C.; Turkyilmaz, M. Reliability of electrode materials for supercapacitors and batteries in energy storage applications: A review. *Ionics* **2021**, *28*, 27–52. [[CrossRef](#)]
123. Deng, T.; Zhang, W.; Arcelus, O.; Kim, J.-G.; Carrasco, J.; Yoo, S.J.; Zheng, W.; Wang, J.; Tian, H.; Zhang, H.; et al. Atomic-level energy storage mechanism of cobalt hydroxide electrode for pseudocapacitors. *Nat. Commun.* **2017**, *8*, 15194. [[CrossRef](#)] [[PubMed](#)]
124. Huang, M.; Li, F.; Dong, F.; Zhang, Y.X.; Zhang, L.L. MnO₂-based nanostructures for high-performance supercapacitors. *J. Mater. Chem. A* **2015**, *3*, 21380–21423. [[CrossRef](#)]
125. Waqas Hakim, M.; Fatima, S.; Rizwan, S.; Mahmood, A. Pseudo-capacitors: Introduction, Controlling Factors and Future. In *Nanostructured Materials for Supercapacitors*; Thomas, S., Gueye, A.B., Gupta, R.K., Eds.; Springer International Publishing: Cham, Switzerland, 2022; pp. 53–70.

126. Herrero, E.; Buller, L.J.; Abruña, H.D. Underpotential Deposition at Single Crystal Surfaces of Au, Pt, Ag and Other Materials. *Chem. Rev.* **2001**, *101*, 1897–1930. [[CrossRef](#)]
127. Brezesinski, K.; Wang, J.; Haetge, J.; Reitz, C.; Steinmueller, S.O.; Tolbert, S.H.; Smarsly, B.M.; Dunn, B.; Brezesinski, T. Pseudocapacitive Contributions to Charge Storage in Highly Ordered Mesoporous Group V Transition Metal Oxides with Iso-Oriented Layered Nanocrystalline Domains. *J. Am. Chem. Soc.* **2010**, *132*, 6982–6990. [[CrossRef](#)] [[PubMed](#)]
128. Yu, G.; Xie, X.; Pan, L.; Bao, Z.; Cui, Y. Hybrid nanostructured materials for high-performance electrochemical capacitors. *Nano Energy* **2013**, *2*, 213–234. [[CrossRef](#)]
129. Gao, D.; Luo, Z.L.; Liu, C.H.; Fan, S.S. A survey of hybrid energy devices based on supercapacitors. *Green Energy Environ.* **2023**, *8*, 972–988. [[CrossRef](#)]
130. Lokhande, C.D.; Dubal, D.P.; Joo, O.-S. Metal oxide thin film based supercapacitors. *Curr. Appl. Phys.* **2011**, *11*, 255–270. [[CrossRef](#)]
131. Yun, Y.S.; Kim, D.H.; Hong, S.J.; Park, M.H.; Park, Y.W.; Kim, B.H.; Jin, H.J.; Kang, K. Microporous carbon nanosheets with redox-active heteroatoms for pseudocapacitive charge storage. *Nanoscale* **2015**, *7*, 15051–15058. [[CrossRef](#)] [[PubMed](#)]
132. Sha, Z.; Zhou, Y.; Huang, F.; Yang, W.M.; Yu, Y.Y.; Zhang, J.; Wu, S.Y.; Brown, S.A.; Peng, S.H.; Han, Z.J.; et al. Carbon fibre electrodes for ultra long cycle life pseudocapacitors by engineering the nano-structure of vertical graphene and manganese dioxide. *Carbon* **2021**, *177*, 260–270. [[CrossRef](#)]
133. Xue, J.Y.; Zhang, F.M.; Ma, W.L.; Wang, M.M.; Cui, H.T. Hierarchically structured nanofelt-like β -NiOOH grown on nickel foam as electrode for high performance pseudocapacitor. *J. Nanopart. Res.* **2015**, *17*, 1–7. [[CrossRef](#)]
134. Kayali, E.; VahidMohammadi, A.; Orangi, J.; Beidaghi, M. Controlling the Dimensions of 2D MXenes for Ultrahigh-Rate Pseudocapacitive Energy Storage. *ACS Appl. Mater. Interfaces* **2018**, *10*, 25949–25954. [[CrossRef](#)] [[PubMed](#)]
135. Cao, L.; Li, H.; Xu, Z.; Zhang, H.; Ding, L.; Wang, S.; Zhang, G.; Hou, H.; Xu, W.; Yang, F.; et al. Comparison of the heteroatoms-doped biomass-derived carbon prepared by one-step nitrogen-containing activator for high performance supercapacitor. *Diam. Relat. Mater.* **2021**, *114*, 108316. [[CrossRef](#)]
136. Wang, Y.; Guo, J.; Wang, T.; Shao, J.; Wang, D.; Yang, Y.-W. Mesoporous Transition Metal Oxides for Supercapacitors. *Nanomaterials* **2015**, *5*, 1667–1689. [[CrossRef](#)]
137. Zhou, Q.; Li, X.; Li, Y.-G.; Tian, B.-Z.; Zhao, D.-Y.; Jiang, Z.-Y. Synthesis and Electrochemical Properties of Semicrystalline Gyroidal Mesoporous MnO₂. *Chin. J. Chem.* **2006**, *24*, 835–839. [[CrossRef](#)]
138. Nayak, P.K.; Munichandraiah, N. Rapid sonochemical synthesis of mesoporous MnO₂ for supercapacitor applications. *Mater. Sci. Eng. B* **2012**, *177*, 849–854. [[CrossRef](#)]
139. Fleischmann, S.; Mitchell, J.B.; Wang, R.; Zhan, C.; Jiang, D.-e.; Presser, V.; Augustyn, V. Pseudocapacitance: From fundamental understanding to high power energy storage materials. *Chem. Rev.* **2020**, *120*, 6738–6782. [[CrossRef](#)] [[PubMed](#)]
140. Cao, Z.; Zhu, Y.-B.; Chen, K.; Wang, Q.; Li, Y.; Xing, X.; Ru, J.; Meng, L.-G.; Shu, J.; Shpigel, N.; et al. Super-Stretchable and High-Energy Micro-Pseudocapacitors Based on MXene Embedded Ag Nanoparticles. *Adv. Mater.* **2024**, *36*, 2401271. [[CrossRef](#)] [[PubMed](#)]
141. Kim, S.K.; Kim, S.A.; Han, Y.S.; Jung, K.-H. Supercapacitor Performance of MXene-Coated Carbon Nanofiber Electrodes. *C* **2024**, *10*, 32. [[CrossRef](#)]
142. Muzaffar, A.; Ahamed, M.B.; Deshmukh, K.; Thirumalai, J. A review on recent advances in hybrid supercapacitors: Design, fabrication and applications. *Renew. Sustain. Energy Rev.* **2019**, *101*, 123–145. [[CrossRef](#)]
143. Kumar, N.; Kim, S.-B.; Lee, S.-Y.; Park, S.-J. Recent Advanced Supercapacitor: A Review of Storage Mechanisms, Electrode Materials, Modification, and Perspectives. *Nanomaterials* **2022**, *12*, 3708. [[CrossRef](#)]
144. Lu, Y.; Zhang, S.; Yin, J.; Bai, C.; Zhang, J.; Li, Y.; Yang, Y.; Ge, Z.; Zhang, M.; Wei, L.; et al. Mesoporous activated carbon materials with ultrahigh mesopore volume and effective specific surface area for high performance supercapacitors. *Carbon* **2017**, *124*, 64–71. [[CrossRef](#)]
145. Seong, K.-d.; Jin, X.; Kim, D.; Kim, J.M.; Ko, D.; Cho, Y.; Hwang, M.; Kim, J.-H.; Piao, Y. Ultrafast and scalable microwave-assisted synthesis of activated hierarchical porous carbon for high-performance supercapacitor electrodes. *J. Electroanal. Chem.* **2020**, *874*, 114464. [[CrossRef](#)]
146. Gao, Y.; Zhang, Y.; Zhang, Y.; Xie, L.; Li, X.; Su, F.; Wei, X.; Xu, Z.; Chen, C.; Cai, R. Three-dimensional paper-like graphene framework with highly orientated laminar structure as binder-free supercapacitor electrode. *J. Energy Chem.* **2016**, *25*, 49–54. [[CrossRef](#)]
147. Yan, Z.; Gao, Z.; Zhang, Z.; Dai, C.; Wei, W.; Shen, P.K. Graphene Nanosphere as Advanced Electrode Material to Promote High Performance Symmetrical Supercapacitor. *Small* **2021**, *17*, 2007915. [[CrossRef](#)]
148. Yang, B.; Chen, J.; Liu, B.; Ding, Y.; Tang, Y.; Yan, X. One dimensional graphene nanoscroll-wrapped MnO nanoparticles for high-performance lithium ion hybrid capacitors. *J. Mater. Chem. A* **2021**, *9*, 6352–6360. [[CrossRef](#)]
149. Chen, P.; Zhou, W.; Xiao, Z.; Li, S.; Chen, H.; Wang, Y.; Wang, Z.; Xi, W.; Xia, X.; Xie, S. In situ anchoring MnO nanoparticles on self-supported 3D interconnected graphene scroll framework: A fast kinetics boosted ultrahigh-rate anode for Li-ion capacitor. *Energy Storage Mater.* **2020**, *33*, 298–308. [[CrossRef](#)]
150. Wang, X.; Sumboja, A.; Khoo, E.; Yan, C.; Lee, P.S. Cryogel Synthesis of Hierarchical Interconnected Macro-/Mesoporous Co₃O₄ with Superb Electrochemical Energy Storage. *J. Phys. Chem. C* **2012**, *116*, 4930–4935. [[CrossRef](#)]
151. Liu, X.; Long, Q.; Jiang, C.; Zhan, B.; Li, C.; Liu, S.; Zhao, Q.; Huang, W.; Dong, X. Facile and green synthesis of mesoporous Co₃O₄ nanocubes and their applications for supercapacitors. *Nanoscale* **2013**, *5*, 6525–6529. [[CrossRef](#)]

152. Hu, T.; Li, J.; Wang, Y.; Chen, S.; Yu, T.; Cheng, H.-M.; Sun, Z.; Xu, Q.; Li, F. Coupling between cathode and anode in hybrid charge storage. *Joule* **2023**, *7*, 1176–1205. [CrossRef]
153. Xu, Y.; Ruan, J.; Pang, Y.; Sun, H.; Liang, C.; Li, H.; Yang, J.; Zheng, S. Homologous Strategy to Construct High-Performance Coupling Electrodes for Advanced Potassium-Ion Hybrid Capacitors. *Nano-Micro Lett.* **2020**, *13*, 14. [CrossRef]
154. Sun, X.; An, Y.; Zhang, X.; Wang, K.; Yuan, C.; Zhang, X.; Li, C.; Xu, Y.; Ma, Y. Unveil Overcharge Performances of Activated Carbon Cathode in Various Li-Ion Electrolytes. *Batteries* **2022**, *9*, 11. [CrossRef]
155. Li, C.; An, Y.B.; Wang, L.; Wang, K.; Sun, X.Z.; Zhang, H.T.; Zhang, X.; Ma, Y.W. Balancing microcrystalline domains in hard carbon with robust kinetics for a 46.7 Wh kg⁻¹ practical lithium-ion capacitor. *Chem. Eng. J.* **2024**, *485*, 149880. [CrossRef]
156. Luo, J.; Zhang, W.; Yuan, H.; Jin, C.; Zhang, L.; Huang, H.; Liang, C.; Xia, Y.; Zhang, J.; Gan, Y.; et al. Pillared Structure Design of MXene with Ultralarge Interlayer Spacing for High-Performance Lithium-Ion Capacitors. *ACS Nano* **2017**, *11*, 2459–2469. [CrossRef] [PubMed]
157. Gao, Y.; Zhou, Y.S.; Qian, M.; Li, H.M.; Redepenning, J.; Fan, L.S.; He, X.N.; Xiong, W.; Huang, X.; Majhouri-Samani, M. High-performance flexible solid-state supercapacitors based on MnO₂-decorated nanocarbon electrodes. *RSC Adv.* **2013**, *3*, 20613–20618. [CrossRef]
158. Wei, W.; Wang, L.; Liang, C.; Liu, W.; Li, C.; An, Y.; Zhang, L.; Sun, X.; Wang, K.; Zhang, H.; et al. Interface engineering of CoSe₂/N-doped graphene heterostructure with ultrafast pseudocapacitive kinetics for high-performance lithium-ion capacitors. *Chem. Eng. J.* **2023**, *474*, 145788. [CrossRef]
159. Wang, L.; Zhang, X.; Xu, Y.N.; Li, C.; Liu, W.J.; Yi, S.; Wang, K.; Sun, X.Z.; Wu, Z.S.; Ma, Y.W. Tetrabutylammonium-Intercalated 1T-MoS₂ Nanosheets with Expanded Interlayer Spacing Vertically Coupled on 2D Delaminated MXene for High-Performance Lithium-Ion Capacitors. *Adv. Funct. Mater.* **2021**, *31*, 2104286. [CrossRef]
160. Amatucci, G.G.; Badway, F.; Du Pasquier, A.; Zheng, T. An Asymmetric Hybrid Nonaqueous Energy Storage Cell. *J. Electrochem. Soc.* **2001**, *148*, A930. [CrossRef]
161. Du Pasquier, A.; Laforgue, A.; Simon, P.; Amatucci, G.G.; Fauvarque, J.-F. A Nonaqueous Asymmetric Hybrid Li₄Ti₅O₁₂ / Poly(fluorophenylthiophene) Energy Storage Device. *J. Electrochem. Soc.* **2002**, *149*, A302. [CrossRef]
162. Li, H.; Cheng, L.; Xia, Y. A Hybrid Electrochemical Supercapacitor Based on a 5 V Li-Ion Battery Cathode and Active Carbon. *Electrochem. Solid-State Lett.* **2005**, *8*, A433. [CrossRef]
163. Khomenko, V.; Raymundo-Piñero, E.; Béguin, F. High-energy density graphite/AC capacitor in organic electrolyte. *J. Power Sources* **2008**, *177*, 643–651. [CrossRef]
164. Bhattacharjee, U.; Bhowmik, S.; Ghosh, S.; Martha, S.K. A perspective on the evolution and journey of different types of lithium-ion capacitors: Mechanisms, energy-power balance, applicability, and commercialization. *Sustain. Energy Fuels* **2023**, *7*, 2321–2338. [CrossRef]
165. Song, S.; Zhang, X.; An, Y.B.; Hu, T.; Sun, C.K.; Wang, L.; Li, C.; Zhang, X.H.; Wang, K.; Xu, Z.C.J.; et al. Floating aging mechanism of lithium-ion capacitors: Impedance model and post-mortem analysis. *J. Power Sources* **2023**, *557*, 232597. [CrossRef]
166. Yi, S.; Wang, L.; Zhang, X.; Li, C.; Liu, W.J.; Wang, K.; Sun, X.Z.; Xu, Y.N.; Yang, Z.X.; Cao, Y.; et al. Cationic intermediates assisted self-assembly two-dimensional Ti₃C₂T_x/rGO hybrid nanoflakes for advanced lithium-ion capacitors. *Sci. Bull.* **2021**, *66*, 914–924. [CrossRef]
167. Wang, P.-L.; Sun, X.-Z.; An, Y.-B.; Zhang, X.; Yuan, C.-Z.; Zheng, S.-H.; Wang, K.; Ma, Y.-W. Additives to propylene carbonate-based electrolytes for lithium-ion capacitors. *Rare Met.* **2022**, *41*, 1304–1313. [CrossRef]
168. Liu, W.J.; An, Y.B.; Wang, L.; Hu, T.; Li, C.; Xu, Y.A.; Wang, K.; Sun, X.Z.; Zhang, H.T.; Zhang, X.; et al. Mechanically flexible reduced graphene oxide/carbon composite films for high-performance quasi-solid-state lithium-ion capacitors. *J. Energy Chem.* **2023**, *80*, 68–76. [CrossRef]
169. Zhou, W.; Liu, Z.; Chen, W.; Zhang, X.; Sun, X.Z.; Luo, M.J.; Zhang, X.H.; Li, C.; An, Y.B.; Song, S.; et al. Thermal characteristics of pouch lithium-ion battery capacitors based on activated carbon and LiNi_{1/3}Co_{1/3}Mn_{1/3}O₂. *J. Energy Storage* **2023**, *66*, 107474. [CrossRef]
170. Jin, L.; Shen, C.; Shellikeri, A.; Wu, Q.; Zheng, J.; Andrei, P.; Zhang, J.-G.; Zheng, J.P. Progress and perspectives on pre-lithiation technologies for lithium ion capacitors. *Energy Environ. Sci.* **2020**, *13*, 2341–2362. [CrossRef]
171. Karthikeyan, K.; Amaresh, S.; Aravindan, V.; Kim, H.; Kang, K.; Lee, Y. Unveiling organic–inorganic hybrids as a cathode material for high performance lithium-ion capacitors. *J. Mater. Chem. A* **2013**, *1*, 707–714. [CrossRef]
172. Krause, A.; Kossyrev, P.; Oljaca, M.; Passerini, S.; Winter, M.; Balducci, A. Electrochemical double layer capacitor and lithium-ion capacitor based on carbon black. *J. Power Sources* **2011**, *196*, 8836–8842. [CrossRef]
173. Wang, L.; Zhang, X.; Kong, Y.-Y.; Li, C.; An, Y.-B.; Sun, X.-Z.; Wang, K.; Ma, Y.-W. Metal–organic framework-derived CoSe₂@N-doped carbon nanocubes for high-performance lithium-ion capacitors. *Rare Met.* **2024**, *43*, 2150–2160. [CrossRef]
174. Ma, Y.; Wang, K.; Xu, Y.; Zhang, X.; Peng, Q.; Guo, Y.; Sun, X.; Zhang, X.; Wu, Z.S.; Ma, Y. Black Phosphorus Covalent Bonded by Metallic Antimony Toward High-Energy Lithium-Ion Capacitors. *Adv. Energy Mater.* **2024**, *14*, 2304408. [CrossRef]
175. Rajalekshmi, A.R.; Divya, M.L.; Lee, Y.S.; Aravindan, V. High-performance Li-ion capacitor via anion-intercalation process. *Battery Energy* **2022**, *1*, 20210005. [CrossRef]
176. Wang, L.; Zhang, X.; Li, C.; Xu, Y.N.; An, Y.B.; Liu, W.J.; Hu, T.; Yi, S.; Wang, K.; Sun, X.Z.; et al. Cation-deficient T-Nb₂O₅/graphene Hybrids synthesized via chemical oxidative etching of MXene for advanced lithium-ion capacitors. *Chem. Eng. J.* **2023**, *468*, 143507. [CrossRef]

177. Wang, L.; Zhang, X.; Li, C.; Sun, X.-Z.; Wang, K.; Su, F.-Y.; Liu, F.-Y.; Ma, Y.-W. Recent advances in transition metal chalcogenides for lithium-ion capacitors. *Rare Met.* **2022**, *41*, 2971–2984. [[CrossRef](#)]
178. Jin, L.; Gong, R.; Zhang, W.; Xiang, Y.; Zheng, J.; Xiang, Z.; Zhang, C.; Xia, Y.; Zheng, J.P. Toward high energy-density and long cycling-lifespan lithium ion capacitors: A 3D carbon modified low-potential $\text{Li}_2\text{TiSiO}_5$ anode coupled with a lignin-derived activated carbon cathode. *J. Mater. Chem. A* **2019**, *7*, 8234–8244. [[CrossRef](#)]
179. Cao, W.; Li, Y.; Fitch, B.; Shih, J.; Doung, T.; Zheng, J. Strategies to optimize lithium-ion supercapacitors achieving high-performance: Cathode configurations, lithium loadings on anode, and types of separator. *J. Power Sources* **2014**, *268*, 841–847. [[CrossRef](#)]
180. Arun, N.; Jain, A.; Aravindan, V.; Jayaraman, S.; Chui Ling, W.; Srinivasan, M.P.; Madhavi, S. Nanostructured spinel $\text{LiNi}_{0.5}\text{Mn}_{1.5}\text{O}_4$ as new insertion anode for advanced Li-ion capacitors with high power capability. *Nano Energy* **2015**, *12*, 69–75. [[CrossRef](#)]
181. Hagen, M.; Cao, W.J.; Shellikeri, A.; Adams, D.; Chen, X.J.; Brandt, W.; Yturriaga, S.R.; Wu, Q.; Read, J.A.; Jow, T.R.; et al. Improving the specific energy of Li-Ion capacitor laminate cell using hybrid activated Carbon/ $\text{LiNi}_{0.5}\text{Co}_{0.2}\text{Mn}_{0.3}\text{O}_2$ as positive electrodes. *J. Power Sources* **2018**, *379*, 212–218. [[CrossRef](#)]
182. Feng, Q.-K.; Zhong, S.-L.; Pei, J.-Y.; Zhao, Y.; Zhang, D.-L.; Liu, D.-F.; Zhang, Y.-X.; Dang, Z.-M. Recent Progress and Future Prospects on All-Organic Polymer Dielectrics for Energy Storage Capacitors. *Chem. Rev.* **2022**, *122*, 3820–3878. [[CrossRef](#)]
183. Zhao, P.; Cai, Z.; Wu, L.; Zhu, C.; Li, L.; Wang, X. Perspectives and challenges for lead-free energy-storage multilayer ceramic capacitors. *J. Adv. Ceram.* **2021**, *10*, 1153–1193. [[CrossRef](#)]

Disclaimer/Publisher’s Note: The statements, opinions and data contained in all publications are solely those of the individual author(s) and contributor(s) and not of MDPI and/or the editor(s). MDPI and/or the editor(s) disclaim responsibility for any injury to people or property resulting from any ideas, methods, instructions or products referred to in the content.